Taylor & Francis
Taylor & Francis Group

Transportmetrica A: Transport Science

ISSN: 2324-9935 (Print) 2324-9943 (Online) Journal homepage: www.tandfonline.com/journals/ttra21

Optimising work zones with enhanced cellular automata and delayed mandatory lane-changing modelling

Yijing Zhao, Bo Wang, Min Zhang, Chi Zhang & Xiazhuo Pan

To cite this article: Yijing Zhao, Bo Wang, Min Zhang, Chi Zhang & Xiazhuo Pan (15 Oct 2025): Optimising work zones with enhanced cellular automata and delayed mandatory lane-changing modelling, Transportmetrica A: Transport Science, DOI: 10.1080/23249935.2025.2571744

To link to this article: https://doi.org/10.1080/23249935.2025.2571744

TRANSPORTMETRICA A: TRANSPORT SCIENCE
https://doi.org/10.1080/23249935.2025.2571744

Optimising work zones with enhanced cellular automata and delayed mandatory lane-changing modelling

Yijing Zhao [a*], Bo Wang [b*], Min Zhang[a], Chi Zhang [b,c] and Xiazhuo Pan[a]

[a]School of Transportation Engineering, Chang'An University, Xi'an, People's Republic of China; [b]School of Highway, Chang'An University, Xi'an, People's Republic of China; [c]Engineering Research Center of Highway Infrastructure Digitalization, Ministry of Education, Xi'an, People's Republic of China

ABSTRACT

In highway work zones, lane-changing behaviour near bottlenecks is more urgent than in general segments, referred to as delayed mandatory lane-changing (DMLC). This study proposes an enhanced cellular work zone automata model (DMLC-EWCA) that incorporates DMLC position probability distribution for micro-simulation. Analysing 12 cases from China, the study shows that lane-changing behaviour varies by lane and is influenced by traffic flow and work zone configuration. Extreme value theory is applied to model DMLC position distribution, and lateral lane-changing rules in DMLC-EWCA are improved. The results highlight that traffic flow, speed, and transition area length are key factors influencing vehicle DMLC position. The DMLC-EWCA outperforms the previous CA model at both microscopic and macroscopic levels. A case study applying the DMLC-EWCA optimised transition area length, enhancing innermost lane usage and overall traffic efficiency. The DMLC-EWCA offers a more accurate approach for modelling traffic flow in work zones.

ARTICLE HISTORY
Received 9 January 2025
Accepted 1 October 2025

KEYWORDS
Work zone; lane-changing behaviour; cellular automata; micro-simulation; transition area optimisation

1. Introduction

Highway work zones introduce lane reductions (Yeom et al. 2018) and traffic bottlenecks (Rayaprolu et al. 2013), causing abnormal traffic behaviours such as sudden braking and mandatory lane-changing (MLC) behaviour, significantly impacting overall road efficiency (Dehman and Farooq 2023; Yeom et al. 2018; Zhang et al. 2012) and safety (Ge and Yang 2020; Zhang, Akinci, and Qian 2023). Between these, MLC behaviour is a significant cause of congestion and accidents in highway work zones (Azam, Bhaskar, and Haque 2022; Toledo, Koutsopoulos, and Ben-Akiva 2003). In work zones, some vehicles maintain their original lane after passing the lane reduction sign and get the visual range of the lane end sign to perform MLC behaviour (Zheng 2014), defined as delayed mandatory lane-changing (DMLC). Due to insufficient lane-changing distance, the DMLC behaviour could easily lead to reduced traffic efficiency (K. Duan et al. 2020). Therefore, understanding and simulating

CONTACT Min Zhang minzhang@chd.edu.cn School of Transportation Engineering, Chang'An University, Xi'an 710000, People's Republic of China

*Yijing Zhao and Bo Wang contributed equally to this work and should be considered co-first authors

DMLC behaviour patterns could identify key factors and develop strategies to mitigate the negative effects of work zones.

Micro-simulation technology could be employed (Hou and Chen 2020) to understand and improve vehicles behaviour in work zones. To reproduce the following behaviour and lane-changing behaviour in work zones, scholars have proposed car-following model (Wiedemann model (Mai, Wang, and Prokop 2019), Gipps model (Vieira da Rocha et al. 2015), GM model (H. Duan et al. 2020), IDM model (Raju et al. 2022)), lane-changing model (Ma and Li 2023), and based on machine learning model (Yifan Zhang et al. 2023). However, traditional models are difficult to describe vehicles interaction behaviour, and machine learning model is difficult to calculate quickly. The cellular automata (CA) model has spatiotemporal discreteness advantage (Nagel and Schreckenberg 1992; Wolf 1999), could capture vehicles interaction behaviour in work zones and relate them to traffic flow characteristics. Early CA models primarily focused on multi-lane traffic flow, where lane-changing rules and vehicle-following behaviours were established to reproduce real-world traffic patterns (Chowdhury, Wolf, and Schreckenberg 1997; Knospe et al. 1999; Zhu, Zhang, and Wu 2015). However, the presence of work zones introduces additional challenges, including lane closures, speed limits, and temporary traffic control measures, which significantly affect traffic efficiency and safety (Fei, Zhu, and Han 2016). To address these challenges, scholars have integrated work zone configurations into CA models, allowing for a more detailed analysis of congestion mechanisms and traffic delay caused by lane reductions and merging bottlenecks (Hou and Chen 2019; Meng and Weng 2011). While these CA models have improved the understanding of work zone traffic flow, they often assume homogeneous vehicle characteristics, neglecting the impact of lane utilisation and lane-changing behaviours. More sophisticated lane-changing mechanisms in CA models have been proposed to account for both aggressive and cooperative driving tendencies, addressing variations in driver decision-making at merging points (Yamauchi et al. 2009). Meanwhile, with advancements in data collection, the emergence of high-resolution trajectory datasets – obtained through GPS tracking, roadside sensors, and unmanned aerial vehicle (UAV) – has provided new opportunities for validating and refining CA models (Cheng et al. 2023; Fukuda et al. 2016; Hou and Chen 2019; Kong et al. 2021; Mallikarjuna and Rao 2011). These datasets allow for the extraction of detailed vehicle behaviour patterns, enhancing the accuracy of longitudinal position updating rules and lateral lane-changing rules in CA model.

This study proposes an enhanced work zone cellular automata (EWCA) model considering the vehicle delayed lane-changing (DMLC) behaviour for one-way three-lane highways. The objectives of this study are: (i) to identify the features of DMLC position and fit its probability distribution by traffic flow characteristics and work zone configurations as covariates from trajectory datasets; (ii) to propose an enhanced work zone cellular automata (EWCA) model to reproduce vehicles behaviour patterns in comparison to the previous CA model; and (iii) to explore the generalisation of the DMLC-EWCA model to improve the work zone configuration in a case study. More precisely, the study addressed the following three questions:

(a) How does the DMLC behaviour pattern change with key influencing factors?
(b) How to develop a work zone CA model to reproduce DMLC behaviour near lane closure locations?

(c) How could the DMLC-EWCA model to develop strategies for mitigating the negative impacts of work zones?

The rest of this study is organised as follows: Section 2 introduces the literature review. Section 3 reports the empirical data in China. Section 4 proposes the DMLC-EWCA model in detail. Section 5 evaluates the simulation results of the DMLC-EWCA model and presents the case study for validation. Finally, conclusions are given in Section 6.

2. Literature review

2.1. The behaviour pattern of work zones

According to the *Road traffic signs and markings* (Standardization Administration of China, 2017), a work zone typically comprises five areas as depicted in Figure 1: advance warning area, transition area, buffer space, activity area, and termination area. This study focuses on the one-way three-lane highway. The closed area is established within the innermost lane and delineated by traffic cones. Vehicles pass through the middle and outermost lanes because of the innermost lane closure. Within the advance warning area, all three lanes remain open for vehicle passage. In the transition area, a taper is set in the innermost lane to facilitate vehicles' lane-changing smoothly into the middle lane. The buffer space is designed to prevent vehicle accidents due to lane-changing failures entering the construction area. The activity area is the actual construction area where entry is prohibited. The termination area allows vehicles to re-enter the previously closed lane and resume normal driving behaviour.

The behaviour pattern of work zones plays a significant role in influencing traffic flow characteristics. Previous studies have examined the vehicles behaviour pattern of different areas in work zones on traffic flow stability, flow-speed, and capacity (Li, Martínez Mori, and Work 2018; Lu et al. 2021; Waleczek et al. 2016; Weng, Meng, and Fwa 2014). As soon as vehicles enter the advance warning area, which is farthest from the work zone, traffic flow is generally stable, with vehicles maintaining a steady following behaviour and relatively small speed fluctuations (Fei, Zhu, and Han 2016; Liu et al. 2024). The traffic density

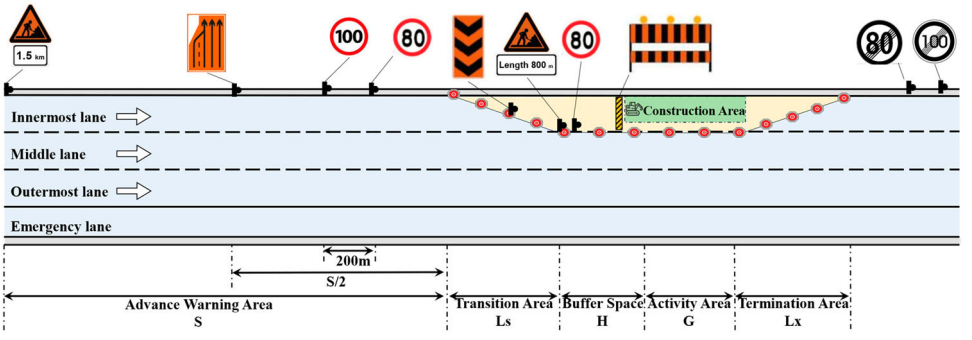

Figure 1. Schematic diagram of work zone with the innermost lane closed in the one-way three-lane highway.

is low, and the vehicles lane-changing behaviour is free like general road sections. Then, as vehicles approach the intermediate of the advance warning area, most vehicles begin to reduce speed and change lane near the lane reduction sign, called mandatory lane-changing (MLC) (Zheng 2014). These behaviour changes cause variations in traffic flow, leading to imbalanced lane utilisation and flow instability (Suh and Yeo 2016; Weng and Meng 2015; Yang et al. 2019). The increased frequency of lane-changing in this area results in uneven lane occupation distribution, which exacerbates flow disturbances and causes localised traffic congestion. However, in the transition area, immediately before entering the lane closure, vehicles behaviour becomes more radicalness. Vehicles are required to complete lane-changing in a limited distance, called delayed mandatory lane-changing (DMLC), leading to rapid accelerations or decelerations. These often result in significant disruptions to traffic flow, including the formation of stop-and-go waves, especially under high traffic volumes (Y. Li, Martínez Mori and Work 2018; Suh and Yeo 2016; W. Zhu, Jia, and Zhao 2010). These findings emphasise the importance of managing lane-changing behaviour, especially DMLC behaviour near the lane closure, to mitigate the adverse effects of work zones on traffic flow. Therefore, understand DMLC behaviour patterns is necessary to capture complex interactions between driver decisions, traffic flow states, and work zone configurations.

2.2. Cellular automata model of work zones

Work zones significantly impact traffic flow due to lane closures, speed reductions, and increased lane-changing activities. The existing cellular automata (CA) models reveals gaps in the modelling and understanding the dynamic mechanism of lane-changing behaviour, starting from mechanical modelling to adapting to heterogeneous traffic flows and incorporating data-driven calibration.

Traditional CA models, such as those proposed by Wolf (1999), generally focus on basic vehicle interactions but fail to capture how lane-changing behaviour evolves as a driver approaches or enters a work zone. These models typically use fixed probabilities for lane-changing, inadequate considering the complexity on behaviour patterns. Then, more sophisticated lane-changing mechanisms have been proposed to engage with CA model (Yamauchi et al. 2009). Meanwhile, to better characterise the influence of heterogeneous traffic flow, research by Kong et al. (2021) and Yang et al. (2019) introduced improvements to account for vehicle-type diversity and different driving behaviours, such as lane-changing dynamics. Recent studies have calibrated and validated CA models. This shift towards data-driven approaches (Cheng et al. 2023; K. Duan et al. 2020; Fei, Zhu, and Han 2016; Fukuda et al. 2016; Hou and Chen 2019; Kong et al. 2021), allowed for more accurate and dynamic simulations that reflect actual traffic conditions. In particular, the ICA model proposed by (Meng and Weng 2011) improved the stochastic deceleration of vehicle longitudinal behaviour from the perspective of probability distribution. These studies highlight that vehicles behaviour pattern is not static and changes depending on factors like the traffic flow and work zone configuration, but lack detailed modelling of how lane-changing behaviour changes along with the distance to lane closure. Therefore, using the data-driven approach to study the detailed lane-changing behaviour along with the distance to lane closure should be included in the CA model.

2.3. The transition area length of work zones

The transition area length plays a crucial role in influencing DMLC behaviour pattern, driving stability, and over all traffic states. Existing research has extensively investigated the influence of transition area length on DMLC behaviour in work zones, primarily from the perspectives of traffic safety and efficiency. These studies have provided valuable insights into how transition area design affects vehicle interactions and overall traffic flow stability. Chen and Tarko (2014) and Kummetha et al. (2020) demonstrated that shorter transition zones lead to increased lane-changing conflicts and crash risks due to constrained maneuvering space. B. Wu et al. (2022) and Difei et al. (2021) further emphasised that insufficient transition lengths force drivers to merge abruptly, increasing turbulence in traffic flow. From an operational perspective, Wang and Lee (2021) and (K. Duan et al. (2022) found that inadequate transition zones contribute to significant speed fluctuations and excessive lateral acceleration, leading to traffic instability and reduced roadway capacity. More recently, S. Ma, Hu, and Wang (2023) highlighted that shorter transition zones heighten driver cognitive workload, leading to increased stress and impaired decision-making, further exacerbating traffic inefficiencies. These findings highlight that transition area length plays a critical role in determining the frequency and pattern of DMLC behaviour, with less emphasis on DMLC behaviour under different traffic states and composition. K. Duan et al. (2020b) has offered controlled environments to analyse DMLC behaviour with driving simulation. However, data-driven approaches to validate the simulation are still limited.

2.4. Research gap

At present, previous studies on work zone traffic behaviour have primarily focused on the impact of transition area length on delayed mandatory lane-changing (DMLC) behaviour from the perspectives of traffic safety and efficiency. There is a lack of systematic analysis on how DMLC behaviour evolves under different traffic states and work zone configurations. Specifically, existing studies have not fully explored the DMLC spatial distribution and their probability characteristics based on empirical trajectory data. Second, existing work zone cellular automata (CA) models often rely on fixed lane-changing probabilities, failing to capture the stochastic and adaptive nature of DMLC behaviour. Additionally, previous CA models have been primarily validated under controlled environments with limited empirical data, restricting their applicability to real-world traffic scenarios. Thus, it is necessary to develop a CA model that integrates empirical trajectory data to improve its adaptability and accuracy in modelling DMLC behaviour.

In order to fill these research gaps, this study proposes an enhanced work zone cellular automata (EWCA) model that explicitly incorporates DMLC behaviour based on trajectory datasets. The obtained empirical data will be used to analyse the spatial distribution and probability characteristics of DMLC under different traffic states and work zone configurations. On this basis, the DMLC-EWCA model will integrate dynamic lane-changing probabilities derived from empirical observations to better reproduce real-world driver behaviour. Furthermore, this study will explore how the DMLC-EWCA model can be applied to optimise work zone configurations (especially transition area length) and mitigate traffic disturbances, ultimately improving traffic management strategies in work zones.

3. Data preparation and preliminary analysis

3.1. Data profile

12 cases were collected from the one-way three-lane highway in China, each lasting approximately 15 minutes (Figure 2). These cases encompass various traffic states allowing for a comprehensive analysis of vehicle behaviour patterns under different levels of traffic demand. The cases have been collected using unmanned aerial vehicle (UAV) video technology to capture and monitor traffic flow. This approach minimises the interference of the monitoring technology on vehicles and accurately reflects vehicles' behaviour. The coverage range of the UAV is roughly 400 m, so that capture the entire work zone in a single shot is challenging. Due to frequent lane-changing behaviour, the advance warning area and transition area are often considered high-risk locations for congestion and accidents. Thus, the video data shooting range mainly contains a partial warning area, transition area, buffer space, and partial activity area.

Upload UAV video to DataFromSky, an open video processing software to identify vehicles and extract trajectories. The DataFromSky Viewer software visualises the trajectory data files in each video frame (30fps). The error of video projection and the plane curve is ignored by using lane marking and centre zoning position as the reference of calibration distance (Gu et al. 2019). The lane widths of cases are 3.75 m obtained from empirical values. Thus, the video cover range and work zone configuration are calculated by the pixel rate which is the ratio of the lane pixel width to the actual width in each video. Then, the traffic flow features and vehicles' trajectories are obtained by DataFromSky Viewer software including vehicle type, traffic volume counts, speed, acceleration/deceleration, and distance. The vehicle size is determined according to the Chinese national standard *GB*

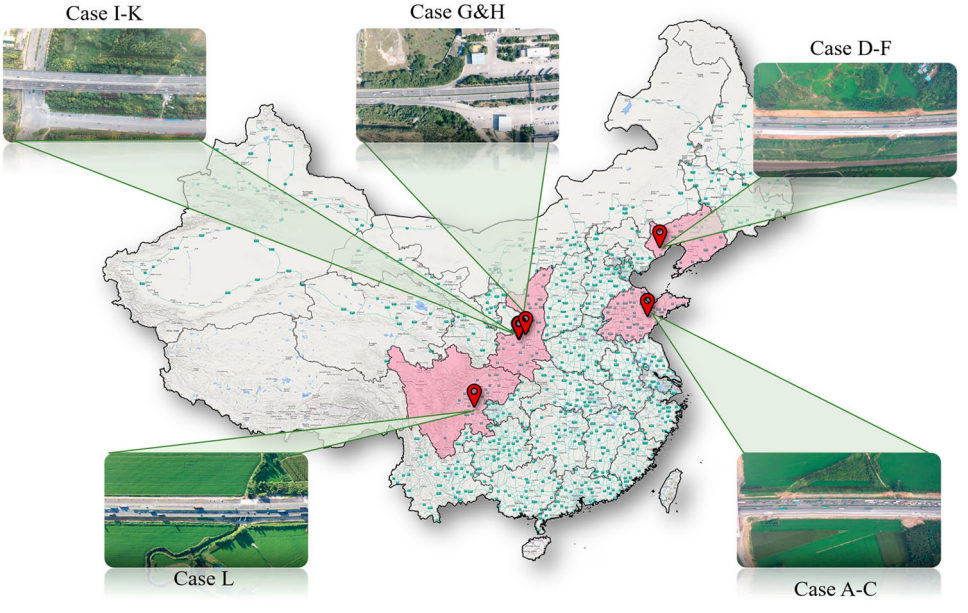

Figure 2. 12 cases were collected on the one-way three-lane highway in China.

Table 1. Work zone features, traffic flow rate, speed, and proportion of heavy vehicles from UAV video.

	Work zone configuration (m)			Traffic flow rate (veh/h)				Speed (km/h)			Proportion of heavy vehicles		
Case	Advance warning area	Transition area	Buffer space and activity area	Q_1	Q_2	Q_3	Q_t	V_1	V_2	V_3	R_1	R_2	R_3
A	183.45	190.31	28.75	900	492	552	1944	38.82	29.68	24.37	0.01	0.44	0.57
B	183.45	190.31	28.75	852	552	540	1944	41.64	34.61	26.81	0.03	0.17	0.51
C	183.45	190.31	28.75	864	540	432	1836	34.36	24.54	20.94	0.00	0.24	0.62
D	287.24	82.53	52.31	792	480	396	1668	83.41	78.94	69.62	0.00	0.47	0.74
E	287.24	82.53	52.31	816	720	372	1908	79.34	76.61	66.71	0.02	0.45	0.85
F	287.24	82.53	52.31	792	696	372	1860	82.25	79.64	67.87	0.03	0.36	0.81
G	213.68	164.72	67.57	483	904	822	2208	62.41	60.54	54.41	0.00	0.37	0.68
H	213.68	164.72	67.57	468	804	768	2040	60.87	62.75	58.36	0.01	0.41	0.63
I	201.83	172.62	34.54	703	978	499	2181	70.54	68.43	58.41	0.01	0.43	0.81
J	201.83	172.62	34.54	710	999	500	2209	65.64	62.57	57.86	0.03	0.46	0.78
K	201.83	172.62	34.54	732	815	439	1986	69.77	68.21	60.09	0.02	0.45	0.85
L	153	225	80	74	126	134	334	90.13	89.36	85.42	0	0.43	0.57

1589–2016: Limits of Dimensions, Axle Load and Masses for Motor Vehicles, Trailers and Combination Vehicles (Standardization Administration of China, 2016). The vehicle type is based on the proportion and size, divided into two types: car and heavy vehicle.

Work zone configuration, traffic flow rate, speed, and heavy vehicle proportions for each lane under normal weather conditions, as shown in Table 1. Q_1, Q_2, and Q_3 represent the traffic flow rate for the innermost, middle, and outermost lanes, respectively, V_1, V_2, and V_3 show the speed of each lane, while R_1, R_2, and R_3 indicate the heavy vehicles' proportion in each lane.

3.2. Preliminary analysis

Vehicle trajectories of cases are extracted to provide insight into the lane-keeping behaviour and lane-changing behaviour of vehicles across different lanes when approaching the closed area. Figure 3 displays individual vehicle trajectories in the innermost, middle, and outermost lanes, respectively. It is evident that vehicles originating from the innermost lane experience the most pronounced lateral fluctuations with all vehicles perform delayed mandatory lane-changing (DMLC) to the middle lane. In contrast, vehicles from the middle lane show relatively mild lane-changing behaviour, with the majority maintaining their lane throughout the segment or initiating earlier, smoother lane-changing.

In order to quantitatively analyse the lateral fluctuation of different lanes along the driving direction, Figure 4 provides error bands of DMLC behaviour by plotting the mean lateral position (solid line) and the corresponding standard deviation (shaded area) for each lane group along the driving direction. This view further confirms the observations from the individual vehicle trajectories. In the innermost lane, the standard deviation increases near the lane closure and then decreases with all vehicles have finished DMLC behaviour to the middle lane. In the middle lane, vehicles exhibit modest deviations from the lane centreline, and the standard deviation increases relatively stable, suggesting more stable lane-keeping behaviour and more evenly distributed DMLC behaviour. In the outmost lane, all vehicles keep moving and the standard deviation is small.

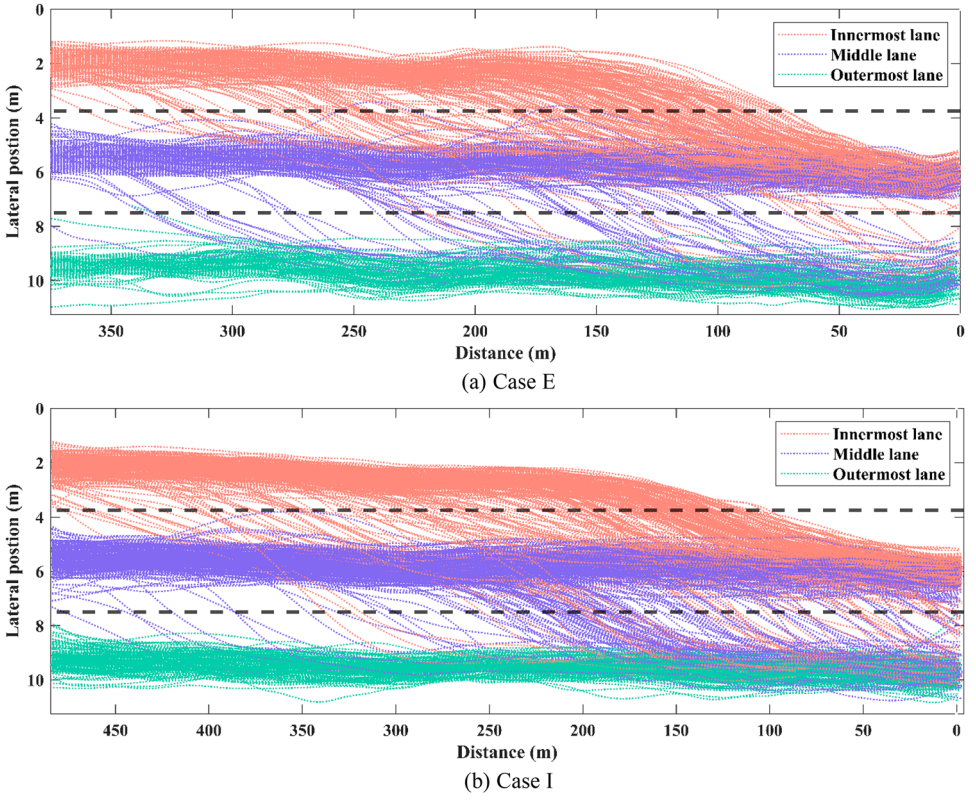

Figure 3. Vehicle trajectories of Case E and Case I (Due to limited space, some cases are presented to illustrate the situation).

Further, the probability of DMLC along the driving direction is analysed to quantitatively demonstrate the differences of each lane. In the innermost lane, the probability of DMLC significant increase near the lane closure and end up at 1 (all completed DMLC). In the middle lane, the probability of DMLC is less than 0.1, which is relatively low and stable. In the outermost lane, the probability of DMLC remains close to the *x*-axis which is 0 and confirms that vehicles in this lane rarely perform DMLC (Figure 5).

To better describe delayed mandatory lane-changing (DMLC) behaviour of the innermost lane, Figure 6 clearly shows each case's central tendency and variability of DMLC positions. The x-axis represents cases, while the *y*-axis indicates the distance from DMLC positions of vehicles to the end of the transition area. Combined with Table 1, the DMLC position distribution is correlated with the work zone configuration (especially the transition zone length) and the traffic flow characteristics (traffic flow and speed), more detailed as follows: (i) The median value of DMLC position indicates the typical distance of vehicles execute their DMLC. The general DMLC position is near the critical area of advance warning area and transition area. When the traffic state is favourable (with traffic speed flow in Table 1 approaching free-flow conditions), vehicles have greater flexibility in lane changing and tend to execute DMLC within the advance warning area (Case D-F & L). As the traffic state deteriorates (with increasing traffic flow rate and

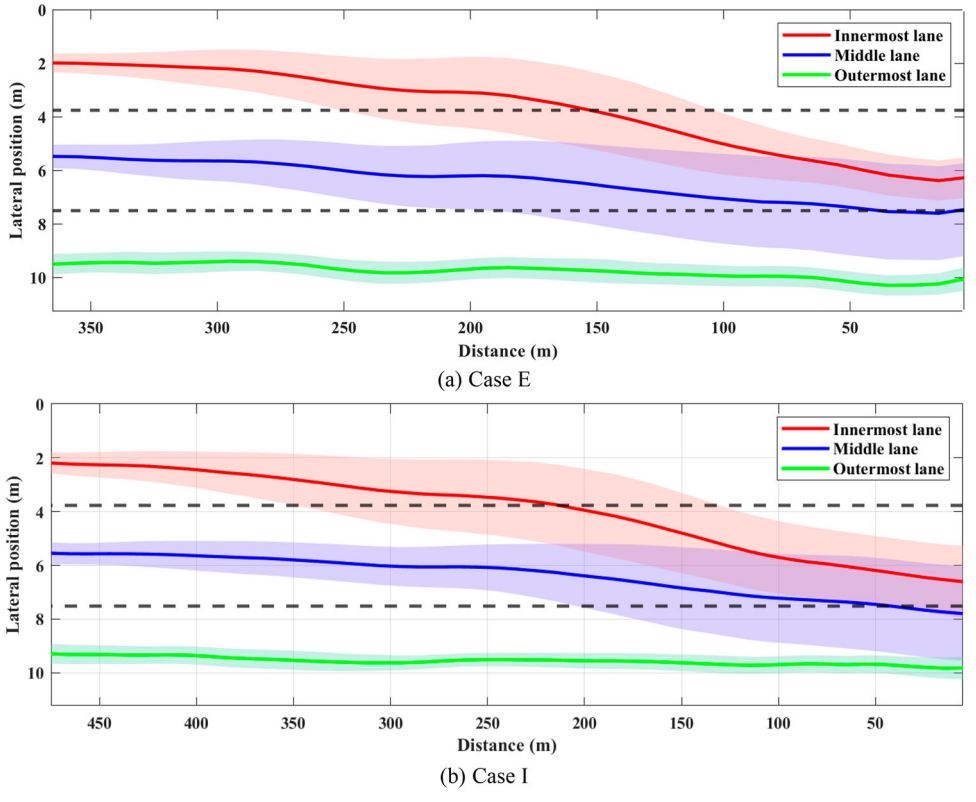

Figure 4. The error band based mean lateral fluctuation and standard deviation in different lanes of Case E and Case I (Due to limited space, some cases are presented to illustrate the situation).

decreasing speed), vehicles are more likely to execute DMLC within the transition area (Case A, B & G-K). When traffic congestion leads to queuing, vehicles experience difficulty in executing lane changes quickly and tend to queue within the advance warning area before completing the DMLC (Case C). (ii) The box height reflects the variability in vehicle DMLC behaviour. A larger interquartile range (IQR) indicates a dispersed phase of DMLC positions, whereas a smaller IQR suggests more consistent DMLC behaviour. Under a favourable traffic state, the distribution of DMLC positions becomes more concentrated, reflecting more uniform lane-changing behaviour among vehicles. When the traffic state deteriorates, the DMLC position distribution becomes more dispersed, as vehicles tend to seek individual opportunities to complete lane changes within a limited space.

DMLC behaviour is an emergency response to the work zone, typically characterised by urgency and unpredictability. Vehicles must execute lane-changing quickly and precisely within a limited time and space. These observations underscore the influence of varying traffic flow features and work zone features of DMLC behaviour, especially in the closed lane. . This study further investigates the characteristics of DMLC behaviour to improve micro-simulation accuracy and better guide work zone layout optimisation.

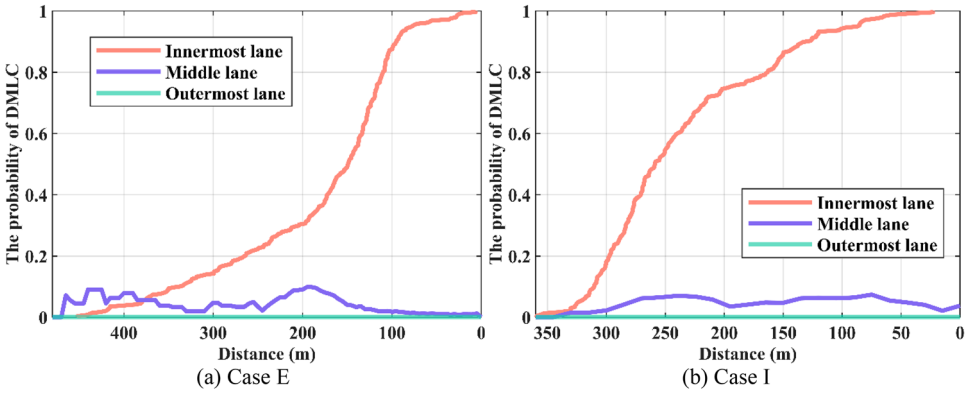

Figure 5. The DMLC probability in different lanes of Case E and Case I (Due to limited space, some cases are presented to illustrate the situation).

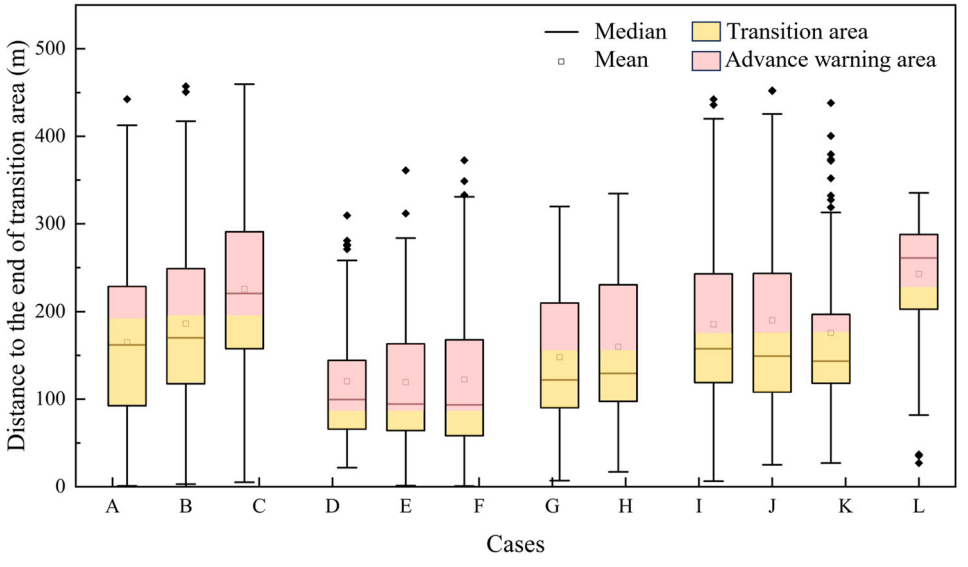

Figure 6. Vehicle delayed mandatory lane-changing (DMLC) positions box diagram.

4. Methodology

4.1. Model framework

This study proposed an enhanced work zone cellular automata (EWCA) model integrating delayed mandatory lane-changing (DMLC) position probability distribution with the innermost lanes closed in a one-way three-lane highway, named the DMLC-EWCA model. Figure 6 illustrates the overall model framework, which consists of two main parts: DMLC position probability distribution determination and DMLC-EWCA model construction. The first part aims to determine the DMLC position probability distribution in the work zone. The first part contains three phases, namely, the DMLC position probability distribution hypothesis, the optimal probability distribution evaluation, and the selection of covariables to fit

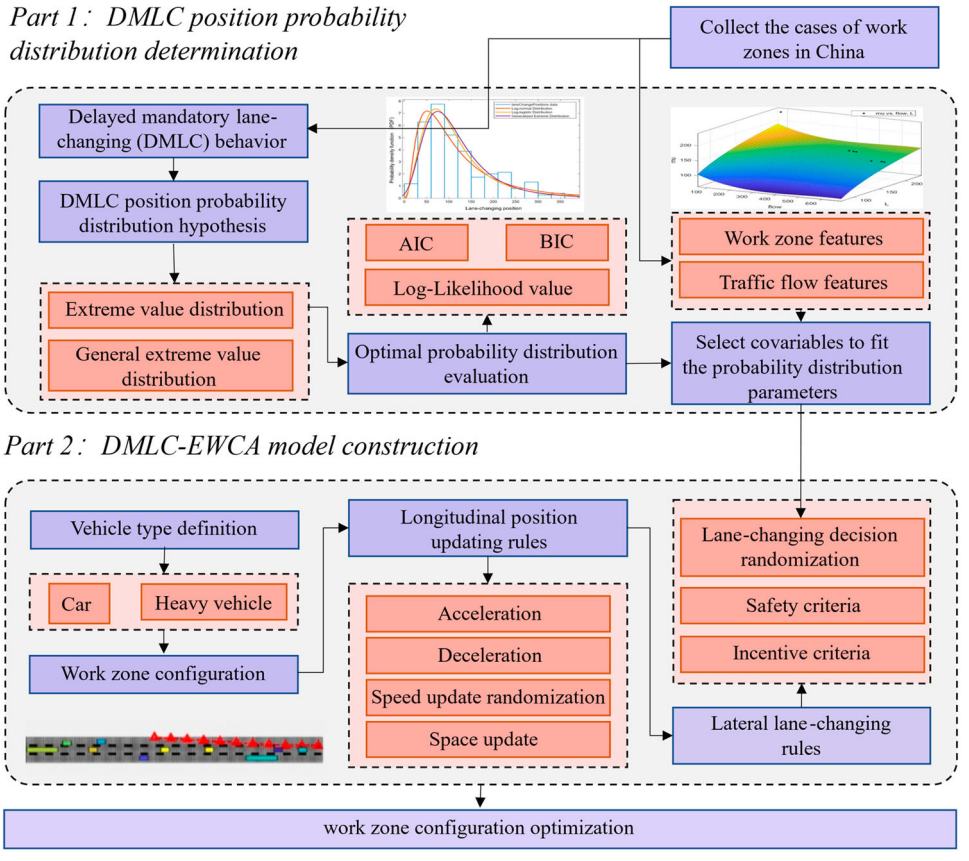

Figure 7. Overall framework of DMLC-EWCA model.

the probability distribution parameters. In this part, the extreme value theory (EVT) is used to assume the probability distribution of the DMLC position. AIC, BIC, and log-likelihood values are selected to evaluate the probability distribution form. Finally, the work zone features and traffic flow features are chosen as covariables to fit the probability distribution parameters. The second part proposes a DMLC-EWCA model with improved lateral lane-changing rules by DMLC position probability distribution. In the second part, the vehicle type in the DMLC-EWCA model is defined according to the actual driving vehicle. Then, the longitudinal position update and lateral lane-changing rules are set. The following subsections are organised as follows. The parts of DMLC position probability distribution determination and DMLC-EWCA model construction, as well as the phases and steps involved in each part (as presented in Figure 7), are introduced in 4.2 DMLC position probability distribution determination, 4.3 DMLC-EWCA model construction in detail, respectively.

4.2. DMLC position probability distribution determination

The innermost lane closure has created a physical bottleneck within the work zone's buffer space and activity area. As vehicles move from the innermost lane to the middle lane in work zones, they must perform mandatory lane-changing (MLC) behaviour. Generally, after the

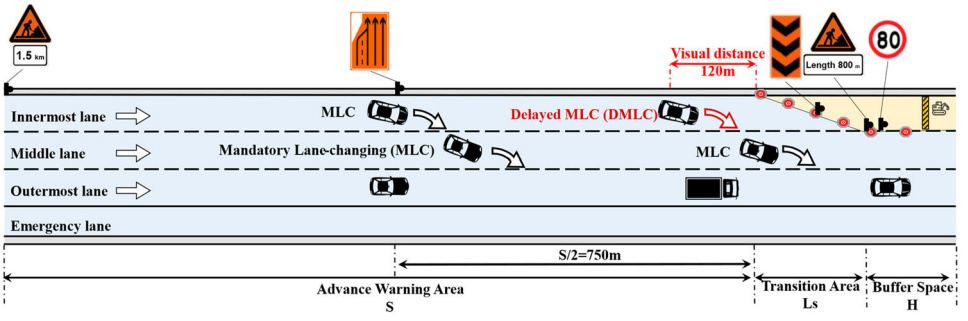

Figure 8. Lane-changing behaviour mechanism in the work zone.

lane reduction sign is placed at the midpoint of the advance warning area, most vehicles execute MLC as intended (Duan et al. 2023). However, a small portion of vehicles, influenced by traffic flow characteristics and randomness, delay their lane change until they reach the visible range of traffic cones. This behaviour is defined as delayed mandatory lane-changing (DMLC), as shown in Figure 8. According to *Design Specification for Highway Alignment* (Ministry of Transport of the People's Republic ofChina, 2017), the visual distance at different design speeds is much shorter than the distance to the midpoint of the advance warning area, highlighting the critical range of DMLC behaviour.

4.2.1. DMLC positions hypothesis

The DMLC behaviour occurs near or within the transition area. Previous studies indicate that DMLC accounts for a low proportion of lane changes upstream of the work zone, which may lead to a sharp increase in traffic accident rates (Huang, Ren, and Meng 2024) and cause congestion when traffic volume increases. Extreme value theory (EVT) focuses on the statistical behaviour of extreme values, which can either be block maxima, such as in the generalised extreme value (GEV) distribution, or peaks over a threshold, as seen in the generalised Pareto distribution. EVT has been widely applied in road safety analysis (Ali, Haque, and Zheng 2023, 2022; Schellander, Lieb, and Hell 2019; Zheng and Sayed 2019), traffic network analysis, and other areas (Oyama, Hara, and Akamatsu 2022). Therefore, DMLC can be considered as the extreme MLC value in the work zone's spatiotemporal dimension upstream. The probability distribution of the DMLC position can be modelled using EVT assumptions.

Generalized Extreme Value Distribution

Suppose $X_1, X_2, \ldots, X_n$ is a sequence of independent random variables with a standard distribution function $H(x)$. X represents the vehicle DMLC position from the innermost lane to the middle lane, and let $M_n = max\{X_1, X_2, \ldots, X_n\}$ corresponds to block maximum. When $n \to \infty$, M_n will converge to a generalised extreme value (GEV) distribution:

$$H(x) = \exp\left\{-\left(1 + k\frac{x-\mu}{\sigma}\right)^{-1/k}\right\}, 1 + \frac{k(x-\mu)}{\sigma} > 0 \tag{1}$$

where, $H(x)$ denotes the GEV distribution function. When the shape parameter $k > 0$, $H(x)$ represents the Type II extreme value distribution (Frechet distribution), with location and scale parameters, respectively. When the shape parameter $k = 0$, $H(x)$ represents the Type I extreme value distribution (Gumbel distribution). When $k < 0$, $H(x)$ represents the Type

III extreme value distribution (Weibull distribution). σ is the scale parameter, and μ is the location parameter.

Extreme Value Distribution

$Z(x)$ denotes the extreme value (EV) distribution function, which could also be called Gumbel distribution. The EV distribution is the GEV distribution when the shape parameter $k = 0$.

$$Z(x) = \exp\left\{-\exp\left[-\left(\frac{x-\mu}{\sigma}\right)\right]\right\} \tag{2}$$

The preceding distribution function reports the probability that the vehicle will change from the closed lane to the adjacent lane (i.e. not survive) before position x. Consequently, the probability that the vehicle will not change from the closed lane to the adjacent lane before position x and therefore survives at least to position x, is represented by the following survival function:

$$S(x) = 1 - F(x) \tag{3}$$

where, $F(x)$ could denotes the GEV distribution function (i.e. $F(x) = H(x)$) or the EV distribution function (i.e. $F(x) = Z(x)$).

The parameters of the above distribution models are estimated using the maximum likelihood estimation (MLE) method.

4.2.2. Optimal probability distribution evaluation

The best probability distribution for fitting the DMLC position could be selected based on (i) evaluating the capability of different distribution models to describe empirical data using the log-likelihood values for parameter estimation; (ii) conducting likelihood ratio tests based on the probability distribution of the phenomena for ordered information criteria (AIC); (iii) considering sample size to provide a larger penalty for the number of parameters in the Bayesian Information Criterion (BIC).

Log-Likelihood value

Log-likelihood is the logarithmic form of the likelihood function for model parameters given the data. A higher log-likelihood indicates a better fit of the model for the data.

$$Log - Likelihood = logL(\theta; X) \tag{4}$$

where, let θ denote the parameters and X the empirical data, with the likelihood function given by $L(\theta; X)$.

Akaike Information Criterion (AIC)

The Akaike Information Criterion (AIC) is a standard used for model selection, taking into account both the log-likelihood of the model and the number of parameters. A lower AIC value indicates a better model.

$$AIC = 2k - 2ln(L) \tag{5}$$

where, k represents the number of probability distribution parameters, and $ln(L)$ denotes the log-likelihood.

Bayesian Information Criterion (BIC)

The Bayesian Information Criterion (BIC) is similar to the AIC but adjusts for sample size, penalising more complex models. A lower BIC value indicates a better model.

$$BIC = ln(n)k - 2ln(L) \tag{6}$$

where, n represents the number of vehicles that perform DMLC.

4.2.3. Regression probability distribution function

Previous studies have analysed the impact of influencing factors on MLC behaviour in work zones from both macroscopic and microscopic perspectives (Hang et al. 2022; Huang, Ren, and Meng 2024; Huang et al. 2023; Li et al. 2024; W. Wu et al. 2022; Zheng 2014). In section 3. Data preparation and preliminary analysis, the DMLC position distribution significantly correlates with traffic flow and work zone features. The transition area length and traffic flow rate related to DMLC behaviour are selected as covariates. In addition, the traffic flow rate could not availably represent the traffic state in work zones, and traffic speed is added as a covariate to characterise the traffic features better. To incorporate the influence of covariates into the modelling process, the parameters of the probability distribution formula are expressed as follows:

$$\omega = h(X^T\beta) \tag{7}$$

$$\sigma = \exp(X^T\beta) \tag{8}$$

where, ω is any of parameters μ, σ and k in the probability distribution function; h is the particular function; X is the covariate matrix; β is parameters vector. To ensure the non-negative of the scale parameters σ, the relationship between σ and covariates is generally represented by an exponential correlation function.

4.3. DMLC-EWCA model construction

An enhanced work zone cellular automata (EWCA) model integrating delayed mandatory lane-changing (DMLC) position probability distribution was proposed.

4.3.1. Grid cell and vehicle feature

Each grid cell measures 1.00 m in length and 0.75 m in width to simulate realistic traffic flow conditions. Each lane horizontally occupies 5 cells with a width of 3.75 m. To account for vehicle composition, weight, size, and impact on traffic flow, we categorise vehicles into two types: cars and heavy vehicles. Based on vehicle dimension and spacing analysis in Table 2, to refine simulation further, cars are modelled as being 3 cells wide and 7 cells long, while heavy vehicles are modelled as being 3 cells wide and 19 cells long.

Table 2. Details of vehicle types.

	Length		Width	
Vehicle type	Actual(m)	Simulation(cell)	Actual(m)	Simulation(cell)
Car	6	7	1.8	3
Heavy vehicle	18	19	2.55	3

4.3.2. Longitudinal position updating rules

An enhanced work zone cellular automata (EWCA) model is used to define longitudinal position updating rules and lateral lane-changing rules, simulating vehicle following and lane-changing behaviours at each time step. In this study, the time step is set to 1s. Vehicles are generated from cases in the real world, with initial states randomly assigned according to the proportion of lane flow and vehicle types. In previous studies, drivers are often divided into radical and cautious types in the longitudinal rules (Cheng et al. 2023; Fei, Zhu, and Han 2016; Zhu, Zhang, and Wu 2015). It is difficult to determine the driver's type in the actual cases, so that calibrate hardly in the CA model. This study takes the longitudinal rules of the ICA model (Meng and Weng 2011) as a reference. The longitudinal position updating rules of vehicles including cars and heavy vehicles, are expressed as follows:

(1) Acceleration:

$$v_n(t) = min(v_n(t) + a,\ v_{max}) \tag{9}$$

(2) Deceleration:

$$v_n(t) = min(v_n(t), d_n) \tag{10}$$

(3) Speed update randomisation with the probability p_l

$$v_n(t+1) = max(v_n(t) - a,\ 0) \tag{11}$$

(4) Space update:

$$x_n(t+1) = x_n(t) + v_n(t+1) \tag{12}$$

where, $v_n(t)$ and $v_n(t+1)$ represent the vehicle speeds at time t and the next time $(t+1)$, respectively, while $x_n(t)$ and $x_n(t+1)$ denote the vehicle positions at those corresponding times. a represents both the acceleration and deceleration of the vehicle, set at 1 m/s⊃2. v_{max} refers to the posted speed limit value at work zone. d_n represents the gap from the front vehicle or traffic cones to the vehicle.

4.3.3. Lateral lane-changing rules

The vehicles' lateral lane-changing rules in the CA model (Fei, Zhu, and Han 2016) are adopted here. In the lateral lane-changing rules, three basic assumptions are made: (i) Once all vehicles start the lane-changing behaviour, they will no longer return to the original lane, and the lane-changing behaviour will stop until they reach the target lane. (ii) All vehicles that do not perform lane-changing behaviour remain in the lane centre all the time. Under a five-cell lane width representation, each vehicle initially occupies the central three cells. (iii) Lane-changing can only be initiated when no vehicles occupy the subject vehicle's projection area onto the target lane.

The lateral lane-changing rules is divided into two phases: the non-lane-changing phase, in which a vehicle remains in its current lane without initiating a maneuver, and the lane-changing phase, in which the vehicle is actively transitioning toward an adjacent lane. A vehicle in the non-lane-changing phase may transition to the lane-changing phase

only when three conditions are satisfied simultaneously: the incentive criterion, the safety criterion, and the lane-changing decision randomisation criterion.

(1) The incentive criterion mainly focuses on the necessary conditions for the vehicle to generate lane-changing motivation. This rule defines the speed and gap of DMLC, based on the relationship between the vehicle performing DMLC and the front vehicle of the target lane.

$$min(v_n(t) + a, v_{max}) > d_n \tag{13}$$

$$d_{front} > d_n \tag{14}$$

where d_{front} represents the shortest forward longitudinal distance in the target lane, measured within the lateral range from the left lane marking to the subject vehicle when projected to the lane centreline, up to the nearest front vehicle in that range. $d_n$is the shortest forward longitudinal distance in the initial lane, measured within the lateral range from the subject vehicle's left boundary to the initial lane marking, up to the nearest front vehicle or lane closure.

(2) The safety criterion focuses on ensuring the safety of vehicles during lane changing. It mainly ensures the gap between the vehicle performing DMLC and the rear vehicle of the target lane.

$$d_{back} > \min(v_{n-1} + a,\ v_{max}) - min(v_n + a,\ v_{max}) \tag{15}$$

where d_{back} represents the shortest backward longitudinal distance in the target lane at the time step, measured within the same lateral projection range of d_{front}, down to the nearest back vehicle in that range. v_{n-1} represents the speed of the nearest vehicle behind in the target lane. Other parameters are the same as those mentioned above.

(3) Lane-changing decision randomisation criterion: This criterion specifies a threshold probability for vehicles at any position x initiate a lane-changing behaviour. A random number $r \sim U(0, 1)$ is generated for each vehicle, and the lane-changing threshold probability of each lane $p_c(n)$ must be exceeded to satisfy this condition.

$$r < p_c(n) \tag{16}$$

$$p_c(n) \begin{cases} F(x), n = 1 \\ 0.1, n = 2 \\ 0, n = 3 \end{cases} \tag{17}$$

where n = 1,2,3 corresponds to the innermost lane, middle lane, and outer lane, respectively. $F(x)$ denotes the DMLC position probability distribution. In previous studies, the lane-changing threshold probability was often a fixed value ($p_c(n) = 0.2$) (Cheng et al. 2023; Fei, Zhu, and Han 2016; Hou and Chen 2019; Meng and Weng 2011). However, in the context of lane-change behaviour in work zones, the closed area necessitates that vehicles on the upstream segment of the innermost lane must execute a lane-change behaviour ($p_c(1) = 1$). Thus, this study gives a more accurate expression of lane-changing randomisation for vehicles in different lanes.

Once all three criterions are satisfied, the vehicle enters the lane-changing phase. In this phase, a vehicle moves laterally by one cell per second, re-evaluating the incentive and safety criterion at each time step. If either criterion is not met, the vehicle temporarily maintains its current lateral offset until the conditions are satisfied again. Under ideal conditions, the maneuver requires 5 seconds (equal to the five-cell lane width); otherwise, it lasts longer until the vehicle reaches the centreline of the target lane, after which it re-enters the non-lane-changing phase and becomes eligible for future lane-changing phase.

4.3.4. Model calibration and validation

Previous studies on CA model calibration have demonstrated that trajectory-based calibration effectively reproduces real-world traffic flow dynamics (Di Pace et al. 2024; Zheng et al. 2023; Zheng et al. 2023). However, the DMLC-EWCA model proposed in this study does not aim to precisely replicate the trajectory of each individual vehicle. Its objective is to capture the longitudinal and lateral behavioural patterns of vehicles under various traffic flow conditions and work zone configurations.

To achieve this, the overall distribution error of DMLC position between empirical data and the simulation results is compared. Specifically, the initial lane position and the DMLC position at the lane boundary in the empirical data are represented as (N, Y), where $N = 1, 2, 3$ corresponds to the innermost lane, middle lane, and outer lane, respectively. Similarly, the DMLC-EWCA model extracts the initial lane positions and DMLC positions of vehicles at the lane boundary using $(N, \hat{Y})$. The vehicles are then sorted based on their longitudinal positions, and the error between the real-world and simulated data is computed sequentially. The vehicles are then sorted based on their longitudinal positions, and the error between the empirical and simulated data is computed sequentially. To eliminate the impact of sign differences in trajectory errors, root mean square error (RMSE) is adopted as the calibration metric. The calibration process is then optimised using a genetic algorithm to enhance model accuracy.

$$minRMSE = \sqrt{\frac{1}{n}\sum_{i=1}^{N}(Y_n - \hat{Y}_n)^2} \tag{18}$$

The DMLC-EWCA model has been validated on both microscopic and macroscopic levels. In the microscopic validation, the delayed mandatory lane-changing (DMLC) positions of vehicles in the innermost lane were compared with empirical data. In the macroscopic validation, the traffic speed of each lane was obtained every 50 m section. And the distribution of lane-changing duration time and longitudinal distance for each lane, using summary statistics and high-quantile agreement to assess fit.

To support these validation metrics, we extract the complete lane-changing process from real trajectories with a simple rule-based threshold method informed by prior work (Yue Zhang et al. 2023). Consecutive crossing frames over a lane marking are detected; the onset of lane-changing is traced forward from the first crossing and the completion lane-changing backward from the second. To prevent misclassifying within-lane jitter as a lane change, trajectories are segmented every 50 m and the mean plus one standard deviation of lateral position among non-changing vehicles in each lane provides data-driven thresholds for onset and completion. For every event, the features are computed by duration

time, longitudinal distance between onset and completion, and related features, enabling consistent micro- and macro-level validation.

5. Result and discussion

5.1. Models

5.1.1. DMLC position probability distribution

The vehicle's delayed mandatory lane-changing (DMLC) position was obtained through the UAV data collected in China. The position probability distribution of DMLC before reaching the end of the transition area of the work zone is extracted. To determine the best type of DMLC position probability distribution, we have adopted extreme value theory (EVT) to construct two distribution functions, including extreme value (EV) distribution and generalised extreme value (GEV) distribution, to describe the probability distribution of DMLC position. The probability distribution parameters estimation of DMLC position is determined by the maximum likelihood estimation method to obtain the probability distribution function of DMLC (from Table A1 in Appendix). We find that:

(a) The location parameter (μ) of the GEV distribution is smaller than that of the EV distribution, indicating that the DMLC position estimated by the GEV distribution is closer to the buffer space and activity area. When comparing μ with the transition area length, the peak of the DMLC position estimated by the GEV distribution falls within the transition area, accounting for the DMLC of the GEV distribution frequently occurring in the transition area.
(b) In terms of the scale parameter (σ), the EV distribution has a larger σ than the GEV distribution. Consequently, the survival function near the peak of the DMLC position in the GEV distribution declines more rapidly than in the EV distribution. This suggests that the DMLC position in the EV distribution is more discrete, while the GEV distribution is more clustered.
(c) The shape parameter (k) is unique to the GEV distribution. A positive k indicates a left-skewed distribution, whereas a negative k indicates a right-skewed distribution. By comparing the k values across various scenarios, it is evident that longer transition area length leads to a DMLC position probability distribution that increasingly approaches a left-skewed distribution. Specifically, when the transition area length is longer, the DMLC position peaks are concentrated at the advance warning area and the start of the transition area; however, with a shorter transition area length, the DMLC position peaks aggregate within the transition area and approach its end.

In general, the lower values for the log-likelihood, AIC, and BIC statistics are preferable. Table A1 in the Appendix gives the statistics of the best-fitted models, showing that the GEV distribution could provide the smallest statistic, providing the smallest values of log-likelihood, AIC, and BIC. Then, the EV distribution has larger parameter estimation errors, especially the shape parameter k, which differs from the GEV distribution. Therefore, the GEV distribution is selected as the probability distribution model to fit the DMLC position.

Table 3. Correlation analysis and calibration results of GEV distribution function.

Parameter	Covariate	Pearson correlation coefficient (r)	P-value	Regression distribution function	R^2
μ	Q	−0.449	0.143	$\mu = 29.74*\exp(0.01*L)$	0.9528
	L	0.927	0.000		
	v	0.036	0.911		
σ	Q	−0.046	0.886	$\sigma = 0.0003*(L^2)\text{-}465.91*(v^{0.04}) + 586.71$	0.9468
	L	0.688	0.013		
	v	−0.686	0.014		
k	Q	0.730	0.007	$k = \text{-}0.0034*L + 0.0010*Q\text{-}0.0092$	0.9707
	L	−0.758	0.004		
	v	0.169	0.600		

5.1.2. Model calibration

To determine the DMLC position probability distribution according to the traffic flow characteristics and work zone configuration, the GEV distribution was used for correlation analysis. Traffic flow Q, traffic speed v, and the transition area length L are selected as covariates. The Pearson Correlation coefficient (r) and P-value between covariates and parameters were calculated. Select significantly correlated covariables to fit the function with the parameters. And R^2 is selected to indicate the parameter fitting quality. The results are shown in Table 3.

From Table 3, it could be found:

(a) The location parameter μ exhibited a strong positive correlation with the transition area length L ($r = 0.927$, $P < 0.001$), indicating that more extended transition areas tend to increase the central tendency of the DMLC position probability distribution. This suggests that vehicles are more likely to adjust DMLC positions further downstream in more extended transition zones, possibly due to improved visual and operational comfort. In contrast, the correlation between traffic flow rate Q and μ, statistically insignificant ($P = 0.143$), implies that the impact of traffic flow on the central tendency of the distribution may be less pronounced under the conditions analysed. Similarly, traffic speed v showed an extremely weak correlation with μ ($r = 0.036$, $P = 0.911$), suggesting that speed fluctuations have little effect on the overall location of the DMLC positions.

(b) Traffic speed v exhibited a significant negative correlation with the scale parameter σ ($r = -0.686$, $P = 0.014$), indicating that higher traffic speeds reduce the variability of DMLC positions. This result is consistent with the notion that higher speeds may limit drivers' decision-making time, leading to more concentrated merging behaviours. The transition area length L demonstrated a significant positive correlation with σ ($r = 0.688$, $P = 0.013$), suggesting that more extended transition areas lead to more dispersed DMLC positions. This is likely due to the increased flexibility provided by extended transition areas. On the other hand, the traffic flow rate Q showed an insignificant and weak negative correlation with σ ($r = -0.046$, $P = 0.886$), suggesting that the volume of traffic has minimal impact on the variability of merging positions under the studied conditions.

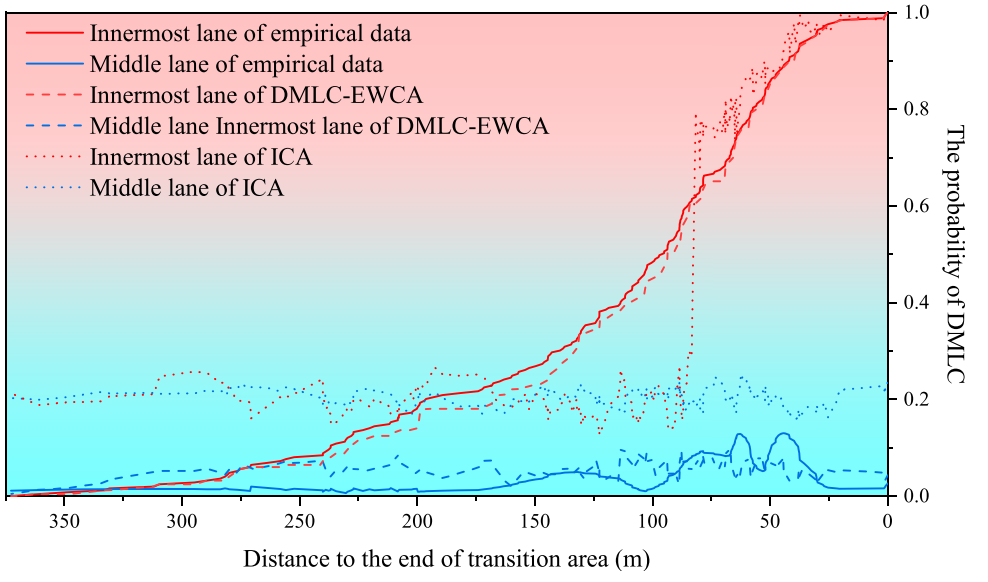

Figure 9. The probability of DMLC over the distance to the end of the transition area. (Comparison among the empirical data, DMLC-EWCA model and improved cellular automata (ICA) model (Meng and Weng 2011)).

(c) The shape parameter k demonstrated strong negative correlations with traffic flow ($r = -0.730$, $P = 0.007$), indicating that lower traffic volumes tend to shift the distribution towards a more left-skewed shape. This implies that under low-flow conditions, drivers tend to change lanes earlier, likely as a risk-averse strategy to avoid conflicts or delays near the transition area end. For the transition area length L, the correlation with k was weak and statistically insignificant ($r = 0.169$, $P = 0.600$), indicating that the length of the merging area does not substantially influence the skewness of the merging position distribution. Some limitations of the study should be pointed out.

The parameters of the DMLC-EWCA model were calibrated with the simulated time step duration of 1 s, as shown in Table 4. Combined with the analysis of empirical data, the traffic flow ratio for vehicle initialisation was set to be Q_1:Q_2:Q_3 = 2:2:1 in the simulation, and the proportion of heavy vehicles was set to be R1 = 0, R_2 = 0.4, and R_3 = 0.8. Meanwhile, the grid cell measures could be used to characterise the longitudinal acceleration of 1 m/s^2 (Cheng et al. 2023) and the lateral acceleration of 0.75 m/s^2 (Siriwardene, Ashraf, and Debnath 2025). By comparing the empirical data, the ICA model (Meng and Weng 2011), and DMLC-EWCA model, the probabilities of DMLC at different lanes as shown in Figure 9. It can be seen that the probability of DMLC position in the previous ICA model was inaccurate. Therefore, in the DMLC-EWCA model, the innermost lane is described by traffic flow, traffic speed and the transition area length according to the GEV distribution function, and the middle lane is defined as 0.1 based on empirical data, which could significantly improve the simulation effect.

Table 4. Calibration results for the DMLC-EWCA model.

Parameter	Description	Results
Cell	The length and width of empirical data	1 m × 0.75 m
Car of cell	The car type is represented by cells	7 × 3 cells
Heavy vehicle of cell	The heavy vehicle type is represented by cells	19 × 3 cells
Traffic flow ratio	The ratio of incoming traffic flow to each lane	By empirical data
Vehicle type proportion	The proportion of vehicles in each lane	By empirical data
Longitudinal position updating rules		
a	Both the following acceleration and deceleration	1 m/s^2
v_{max}	The maximum limited speed at work zones	By empirical data
p_l	The probability of speed update randomisation	0.3
Lateral lane-changing rules		
p_{c1}	The probability of DMLC in the innermost lane	By GEV distribution function
p_{c2}	The probability of DMLC in the middle lane	0.1
a_c	The lateral acceleration of DMLC	0.75 m/s^2
v_{max}	The maximum limited speed at work zones	By empirical data
minRMSE	The objective function of DMLC-EWCA model	2.8175

5.1.3. Model validation

In microscopic validation, the positions of delayed mandatory lane-changing (DMLC) in the innermost lane were analysed. Figure 10 demonstrates the progressive improvement in predicting the lane-changing position distribution as the CA model evolved from the ICA model proposed by Meng and Weng (2011) to the DMLC-EWCA model. The previous CA model exhibited a significant deviation in capturing the spatial distribution of lane-changing behaviour, particularly underestimating high frequencies in the transition area (Pearson = 0.7036). In contrast, the DMLC-EWCA(a) model notably enhanced the prediction accuracy (Pearson = 0.9391). Subsequent refinements led to further improvements, culminating in the DMLC-EWCA model, which demonstrated the highest similarity (Pearson = 0.9671). These results highlight the DMLC-EWCA ability to effectively capture lane-changing behaviour, particularly in the transition area, and emphasise the significant advancements achieved through iterative improvements.

In macroscopic validation, Figure 11 compares the traffic speed results simulated by the DMLC-EWCA model, the ICA model proposed by Meng and Weng (2011), and empirical data across three different areas: the advance warning area, the transition area, and the buffer space. Traffic speed data for each lane were collected in 50-meter segments and averaged over 15 minutes of continuous traffic flow. The Root Mean Square Error (RMSE) between the empirical data and the simulation models is provided to quantify the simulation accuracy for each lane.

From Figure 11, the proposed DMLC-EWCA model is validated and reveals the following main findings:

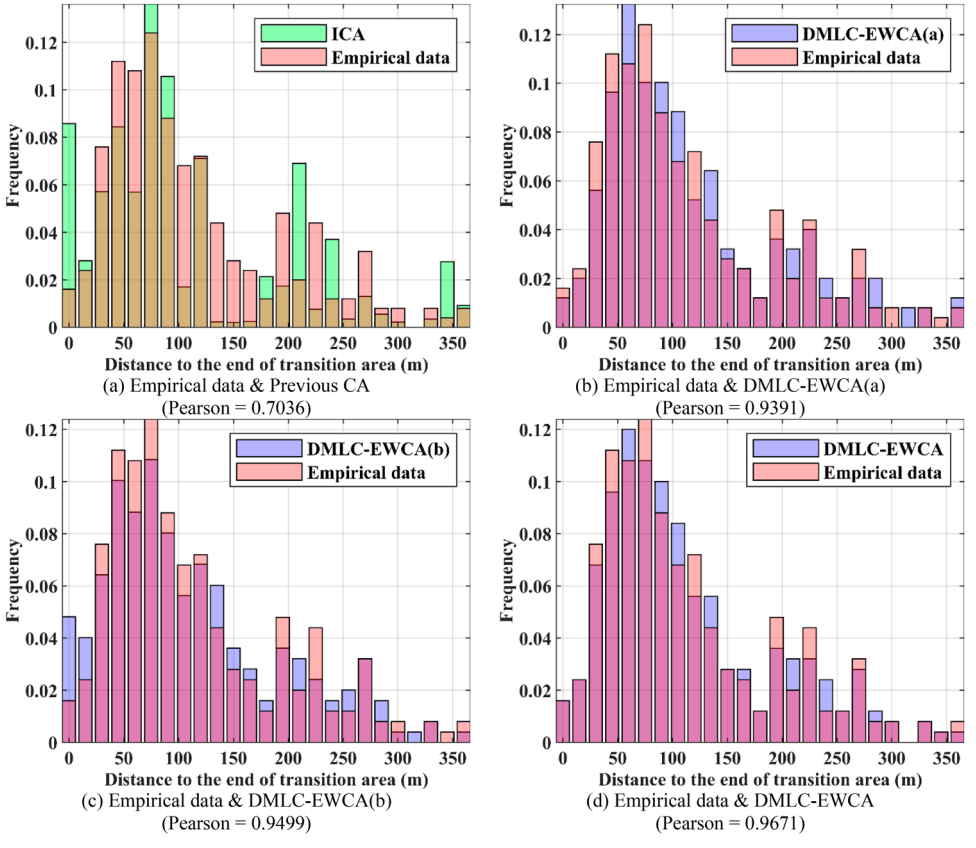

Figure 10. DMLC position distribution comparison between the empirical data of cases and the simulation results. (a) Comparison between the empirical data and the ICA model proposed by Meng and Weng (2011). (b) Comparison between the empirical data and DMLC-EWCA(a) which improves the lateral lane-changing probability of the innermost lane. (c) Comparison between the empirical data of cases and DMLC-EWCA(b) which improves the lateral lane-changing probability of the middle lane on the previous basis. (d) Comparison between the empirical data and DMLC-EWCA which improves the grid cell measure on the previous basis.

(a) In the advance warning area, traffic signals or signs are typically placed to alert drivers of the approaching closed area. Although vehicles start to experience some disruption, the speed change is not drastic and generally remains relatively high.

(b) In the transition area, lanes gradually shift to the closed area due to construction. The speed decreases gradually and fluctuates from the normal driving state, which reflects the adjustment process of traffic flow instability (Jiang et al. 2017). The DMLC-EWCA model, considering delayed mandatory lane-changing (DMLC) behaviour, effectively simulates the speed reduction because of increased traffic density as the lane closure.

(c) The buffer space typically experiences higher traffic flow and relatively lower speeds. Due to the continued impact of the closed area, vehicles may maintain lower speeds. The traffic flow in buffer space and activity area remains relatively stable but is significantly lower than normal driving conditions. The simulation results from the

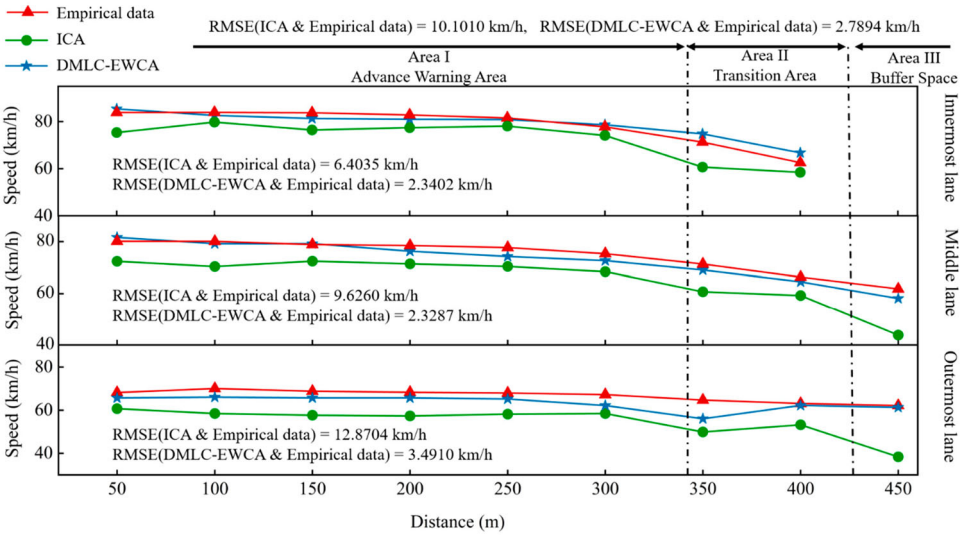

Figure 11. Traffic speed comparison between the simulation and the empirical data.

DMLC-EWCA model are consistent with the measured data, maintaining a lower level of speed.

(d) From the empirical data indicates that the closed area has a lesser impact on lanes farther from the closure (i.e. the outermost lane). The DMLC-EWCA performs well in simulating speed trends in the innermost and middle lanes but is less accurate for the outermost lane (RMSE = 3.4910 km/h). This limitation may arise because the DMLC-EWCA primarily focuses on improving the DMLC probability distribution between the closed lane (innermost lane) and the adjacent lane (middle lane). However, the DMLC-ECA's speed predictions closely match empirical data, highlighting the importance of incorporating lane-changing behaviour of each lane to enhance simulation accuracy in the bottleneck (RMSE from 10.1010 km/h to 2.7894 km/h).

Moreover, empirical data shows that lane-changing behaviours in work zones occur on the innermost lane and middle lane. Therefore, the complete lane-changing process was extracted from the empirical data and compared with the simulation results of DMLC-EWCA as shown in Table 5.

For both lane-changing duration time and the longitudinal distance, the means and 85th percentiles align well between simulation and empirical data. This agreement at the central tendency indicates that the DMLC-EWCA model could statistically reproduce typical lane-changing behaviour across different lanes (two-sided Mann–Whitney U tests, all $p > 0.05$). But lager discrepancies arise at the extremes: the simulated minimum and maximum span a narrower range than empirical data. This gap is attributable to two simplifications in the current implementation. First, the cellular partitioning imposes spatial–temporal quantisation, which compresses very short and very long behaviours. Second, the lateral dynamics are simplified by using a fixed lane-change acceleration, which limits variability and cannot capture the full dynamic evolution of real lane-changing. Consequently, the DMLC-EWCA

Table 5. Lane-changing process comparison between the DMLC-EWCA model and empirical data.

		Empirical data		Simulated results	
		Innermost lane	Middle lane	Innermost lane	Middle lane
Lane-changing duration time (s)	Minimum	2.93	2.50	5	5
	Mean	5.82	4.93	5.94	5.39
	85th percentile	7.26	5.76	7	6
	Maximum	15.2	12.97	9	9
	P value (U test)	/	/	0.681	0.874
Longitudinal distance of lane-changing process (m)	Minimum	29.16	17.08	19	16
	Mean	110.12	81.37	97.65	69.42
	85th percentile	126.10	112.98	119.54	98.54
	Maximum	223.12	255.73	203	193
	P value (U test)	/	/	0.276	0.179

model under-represents extreme durations and distances while still matching the typical behaviour.

5.2. Impacts of transition area length

The variation of traffic flow in buffer space and activity area with the increasing length of the transition area and lane occupancy demonstrates a distinct trend as depicted in Figure 12. The colour gradient in the figure illustrates traffic flow values ranging from 0 (blue) to over 2000 (red). Overall, peak traffic flow is predominantly observed in the moderate lane occupancy range (red region), while extreme conditions (low or high lane occupancy) correspond to significantly reduced traffic flow (blue regions). This trend further confirms the importance of maintaining moderate lane occupancy for efficient traffic flow management.

The effect of transition area length (Ma, Hu, and Wang 2023; Morgan, Duley, and Hancock 2010) on traffic flow distribution appears to be relatively limited in the lower lane occupancy and remarkable in the higher lane occupancy (Zhang et al. 2020). Across various lengths, the peak traffic flow consistently occurs within the moderate lane occupancy range. However, at shorter transition area lengths (e.g. around 50 m–100 m), the probability distribution of traffic flow exhibits a more concentrated pattern, suggesting that shorter transition areas impose stronger constraints on the traffic flow distribution (Ma, Hu, and Wang 2023). This indicates that the design of the transition area length has some degree of flexibility, allowing for adaptation to specific spatial constraints without significantly compromising traffic efficiency.

Figure 13 illustrates the variation of traffic speed in buffer and activity areas with the increasing length of the transition area and lane occupancy. At low lane occupancy levels (approximately 0.2–0.4), traffic speed is high, reaching values close to 90 km/h (green region). As lane occupancy increases toward full capacity (0.8–1.0), traffic speed decreases sharply, falling below 10 km/h in extreme cases (red region). This trend underscores the inverse relationship between lane occupancy and traffic speed, suggesting that higher lane occupancy leads to significant congestion and reduced operational efficiency.

The transition area length also plays a role in modulating the traffic speed of buffer space and activity area. Across all lane occupancy levels, more extended transition areas

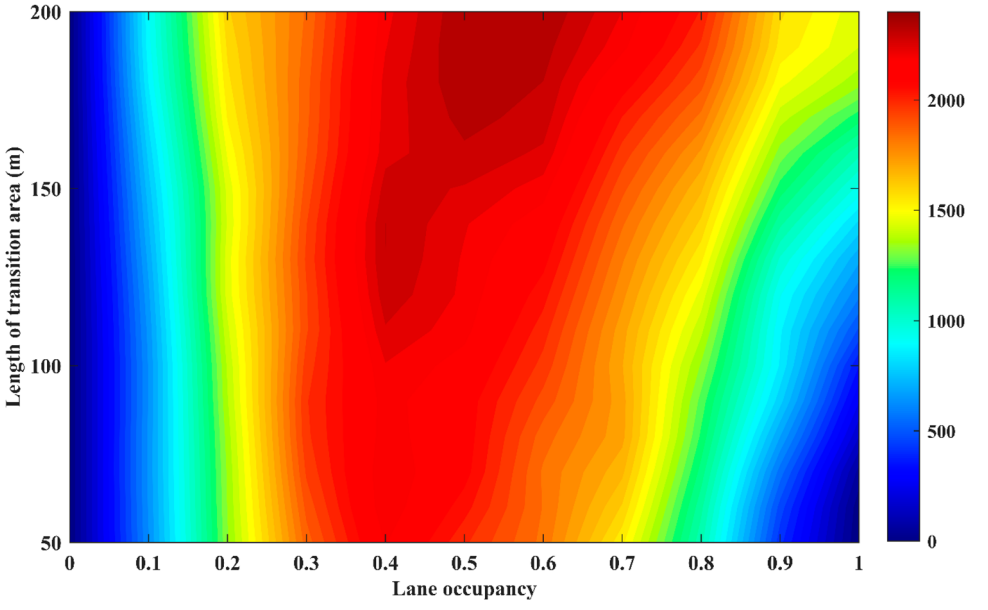

Figure 12. Traffic flow of buffer space and activity area with the increasing length of the transition area and lane occupancy.

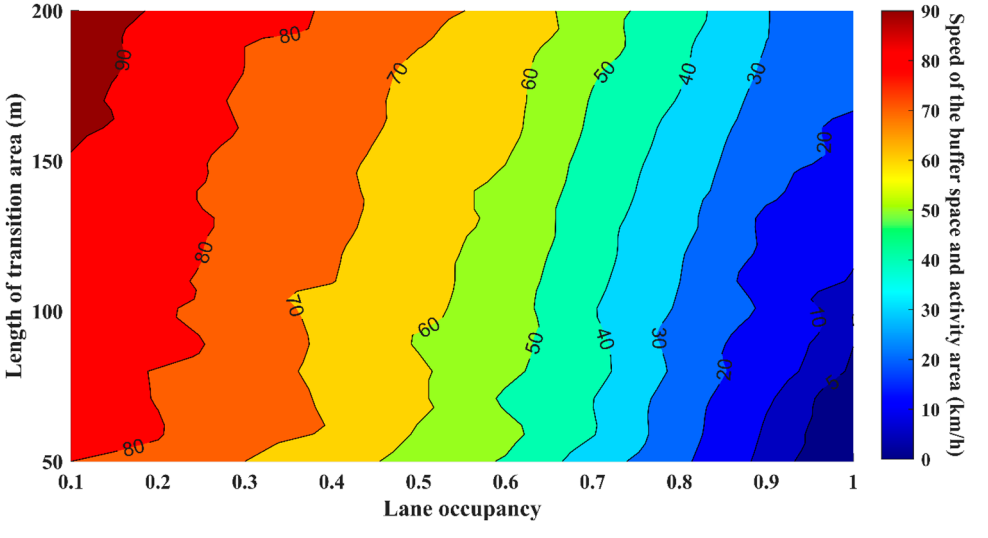

Figure 13. Speed of the buffer space and activity area with the increasing length of the transition area and lane occupancy.

(150–200 m) are associated with slightly higher speeds compared to shorter transition areas (50–100 m) (Ma, Hu, and Wang 2023). For instance, under moderate lane occupancy conditions (0.5–0.7), traffic speed ranges from 40 to 60 km/h in longer transition areas, whereas shorter transition areas exhibit slightly lower speeds. This indicates that longer transition areas may alleviate congestion by providing smoother vehicular flow.

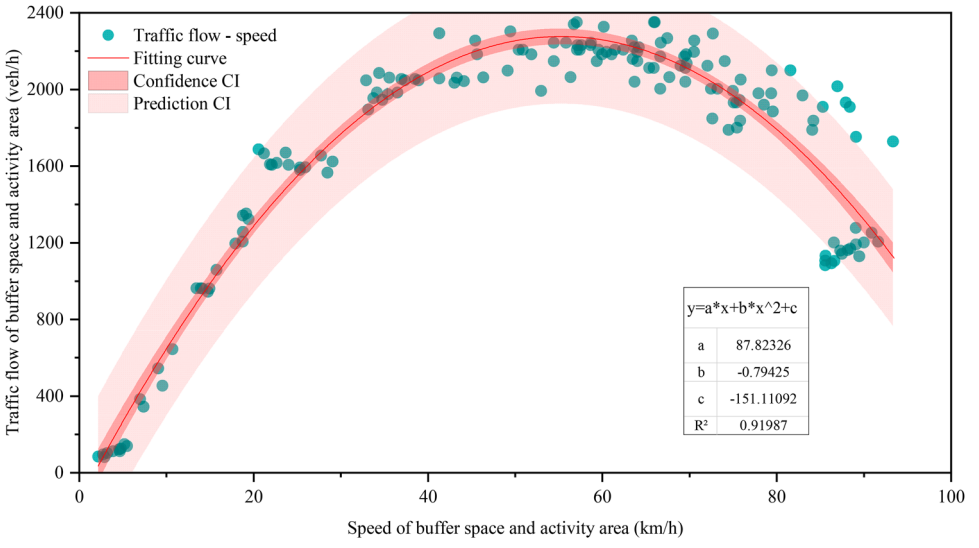

Figure 14. Traffic flow – Speed relationship of DMLC-EWCA model.

Figure 14 illustrates a parabolic relationship between the traffic speed and traffic flow in buffer and activity areas, reflecting the classical traffic flow-speed relationship. The validity of the DMLC-EWCA model is further illustrated. Traffic flow is relatively low at low speeds (below 20 km/h), with traffic flow below 500 veh/h. As speed increases, traffic flow rises steadily. At a speed of 60–70 km/h, the traffic flow of buffer space and activity area could reach a maximum of approximately 2,200 veh/h, the traffic capacity with the innermost lane closed in a one-way three-lane highway. The traffic capacity value obtained by the DMLC-EWCA is approximately consistent with the simulation results of Cheng et al. (2023). However, the results of (Cheng et al. 2023) did not explicitly discuss the change of traffic capacity in the buffer space and activity area under different conditions and this study added.

5.3. Case study

5.3.1. Case study overview and DMLC-EWCA modelling

To apply the DMLC-EWCA model, a case study is presented to optimise the length of the transition zone in the work zone. The case study is Case E from the G1 highway in Liaoning Province, China, which has three lanes in each direction, and the designed speed is 120 km/h, as shown in Figure 15(a). To model and analyse traffic flow in the work zone, a DMLC-EWCA model by MATLAB is developed Figure 15(b). The lanes are discretized into uniform cells, each representing a small segment of road space, and vehicles occupy cells depending on their position. The DMLC-EWCA model incorporates key features such as work zone configuration, vehicle type proportion, specific speed limits, stochastic lane-changing behaviour, and boundary conditions reflecting upstream inflow.

Additionally, the DMLC-EWCA model captures non-linear traffic dynamics caused by lane closures, enabling accurate simulation of congestion propagation and providing a foundation for traffic efficiency evaluation and optimisation. Figure 16 compares Case E's

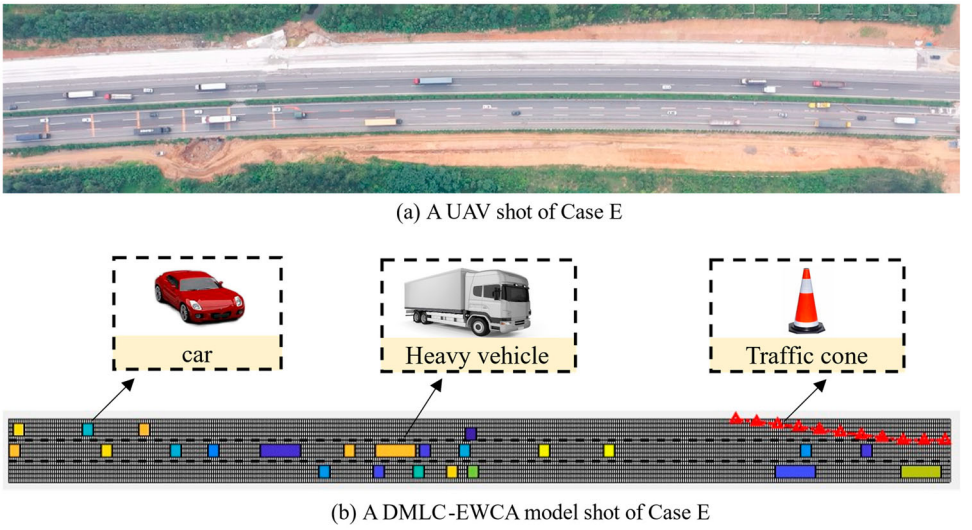

(a) A UAV shot of Case E

(b) A DMLC-EWCA model shot of Case E

Figure 15. The DMLC-EWCA model of Case E.

spatial–temporal trajectory diagrams and the DMLC-EWCA model simulation results for each lane, with vehicles' speed represented by a colour gradient (40–90 km/h). Significant differences in speed variations over time can be observed across different lanes. The DMLC-EWCA model demonstrates high predictive accuracy in replicating the complex traffic dynamics observed in the real world. Specifically, the DMLC-EWCA model effectively captures the variations in lane-changing behaviour, vehicle density, speed distributions, and lane usage patterns across the innermost, middle, and outermost lanes. The consistency in trajectory trends, including congestion propagation and recovery phases, highlights the capability of the DMLC-EWCA model to accurately simulate complex vehicles' behaviour in highway work zones. These results validate the DMLC-EWCA model as a reliable tool for analysing and optimising traffic flow in work zones. However, the DMLC-EWCA model provides a more balanced and efficient traffic flow across all lanes compared to Case E in real word. This is because the upstream traffic flow input of work zones in the real world is random and disorderly.

5.3.2. Case study improvement

According to Section 5.2 Impacts of transition area length, the adjustment of the transition area length was informed by the traffic flow and speed of the bottleneck area (the buffer space and activity area). According to the conversion relationship between the traffic flow rate in Case E and lane occupancy in DMLC-EWCA model (Cheng et al. 2023), the lane occupancy is about 0.2 in DMLC-EWCA. From Figure 12, the traffic volume in the bottleneck area does not change significantly, with 50–150 m in the length of the transition area. At about 150 m, the bottleneck area's traffic flow increased and stabilised. Then, in the same lane occupancy, the extended length of the transition area results in higher speed in the bottleneck area. Consequently, the adjusted length of the transition area in Case E (150 m, as shown in Figure 17) was determined to balance operational efficiency. The

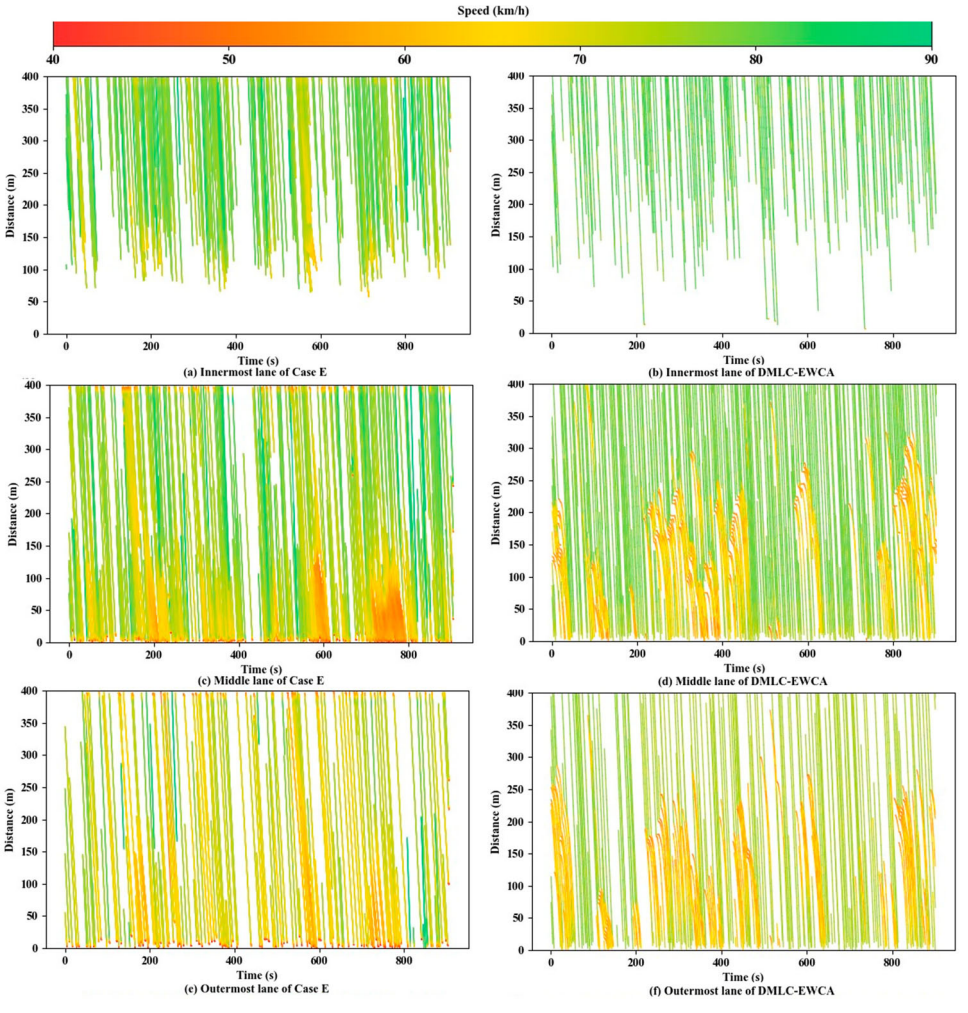

Figure 16. Spatial-temporal trajectory diagram of the traffic flow on each lane.

adjusted transition area length and associated traffic flow parameters were soon validated in DMLC-EWCA.

The improved length of the transition area results from the DMLC-EWCA model, as shown in Figure 18, demonstrate that adjusting the transition area length significantly improves the traffic flow within the work zone. Especially in the outermost and middle lanes, the extended transition area reduces the severity of stop-and-go waves, leading to smoother vehicle trajectories and a more gradual lane-changing process. Then, the adjusted length of the transition area improves the use of the innermost lane. Moreover, the speed distribution across lanes reflects typical traffic behaviour, with the innermost lane maintaining better flow efficiency. These findings underscore the critical role of optimising transition zone length in alleviating congestion and enhancing traffic flow efficiency in work zones, providing valuable insights for traffic management strategies in similar scenarios.

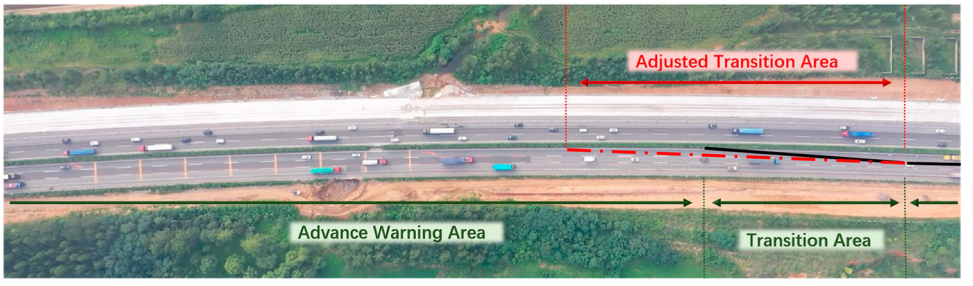

Figure 17. The length of the transition zone is improved in Case E.

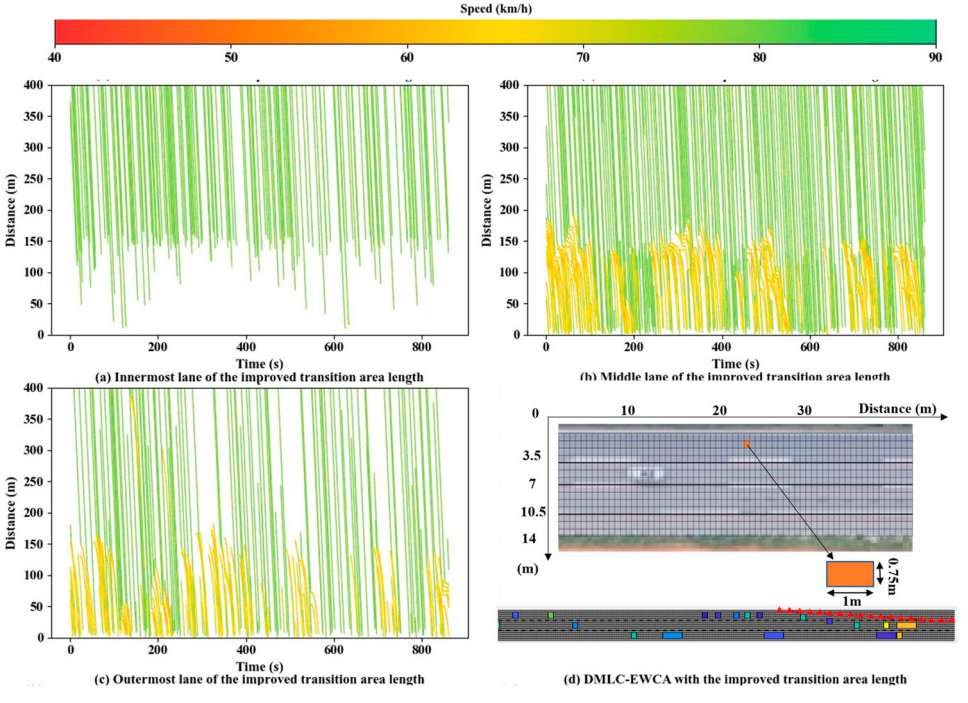

Figure 18. Spatial-temporal trajectory diagram of the improved transition area length by DMLC-EWCA.

6. Conclusion

In this study, a DMLC-EWCA model was proposed to address the specific challenges posed by lane-changing behaviour in highway work zones, particularly near the transition area where is most prevalent. The model incorporates lane-changing behaviour on each lane and considers key factors such as traffic flow, speed, and transition area length by case data from Chinese highways. Based on the findings, the following primary conclusions are drawn:

(1) The DMLC position probability distribution is identified by the Generalized Extreme Value (GEV) distribution as the most suitable model through Extreme Value Theory

(EVT). Compared to the Extreme Value (EV) distribution, the GEV distribution provides a better fit with smaller values for log-likelihood, AIC, and BIC statistics. The analysis reveals that the location parameter of the GEV distribution is positively correlated with the length of the transition area, suggesting that longer transition areas shift the DMLC specific position downstream, which is consistent with the trends observed in the real-world data from China.

(2) Regression analysis reveals significant effects of transition area length on the DMLC position distribution. More extended transition areas lead to more concentrated DMLC positions, while shorter transition areas increase the variability of the distribution. Traffic flow and speed also influence the scale and skewness of the DMLC position distribution. Specifically, higher traffic speeds reduce the variability of DMLC positions, while lower traffic flow tends to shift the distribution toward a left-skewed shape. These findings align with the traffic conditions observed in China's highway networks, further validating the model's applicability to real-world scenarios.

(3) Both microscopic and macroscopic validation of the DMLC-EWCA model demonstrate its higher accuracy in predicting lane-changing positions (Pearson from 0.704 to 0.967) and traffic speed variations (RMSE from 10.101 km/h to 2.789 km/h) compared to the ICA model proposed by (Meng and Weng 2011). The DMLC-EWCA model effectively simulates the rules of lane-changing behaviours and the decrease in speed within transition areas, providing a more accurate prediction of traffic dynamics. The validation results, consistent with case data collected in China (two-sided Mann–Whitney U tests, all $p > 0.05$), underscore the model's robustness and suitability for traffic flow analysis in work zones.

(4) A case study applying the DMLC-EWCA model shows that optimising the transition area length significantly improves traffic flow within the work zone and reduces congestion. The extended transition area mitigates the severity of stop-and-go waves, resulting in smoother vehicle trajectories and more gradual lane-changing processes. This improvement enhances traffic flow efficiency, particularly in the innermost and middle lanes. The findings emphasise the critical role of optimising transition zone design in alleviating congestion and improving traffic flow in work zones, providing valuable insights for traffic management strategies in similar scenarios.

Some limitations of this study should be pointed out. First, this study focused on the one-way three-lane highways with the innermost lane closed. Thus, the number of other lanes and the form of other lanes closed could not apply. In the future, it should be worth exploring the vehicle's lane-changing behaviour in all forms of work zones to refine the DMLC-EWCA model. Second, the UAV could not cover the whole work zone, especially in the advance warning area. It is difficult to capture the complete vehicle lane-changing trajectory within the work zone in the real world. It would be suggested that more technologies (e.g. driving simulators) be used to obtain the full interactive behaviour of vehicles. Last, although the DMLC-EWCA model takes into account the traffic volume, speed, vehicle position, and dynamic interactions with surrounding vehicles, it has limitations in simplified vehicle the intra-maneuver dynamics of lane-changing. Once a lane change is initiated, the lateral motion proceeds without time-varying acceleration or driver-specific variability,

and the maneuver continues until the target lane is reached with no possibility of cancellation. But in real-world traffic, drivers may abort lane-changes in response to sudden traffic fluctuations, interactions with surrounding vehicles, or changes in perceived safety. Future work should incorporate this mechanism by modelling its triggering conditions, probabilistic characteristics, and operational impacts, thereby enhancing the CA model's ability to represent realistic driving behaviour.

Disclosure statement

No potential conflict of interest was reported by the author(s).

Funding

This work was supported by the Xi'an Social Science Planning Fund Project (No. 25GL123), the Special Project for Serving the Local Area of the Shaanxi Provincial Education Department (No. 24JE005), and the Science and Technology Project of the Sichuan Transportation Department (No. 2023-A-10).

ORCID

Bo Wang https://orcid.org/0000-0002-0593-6612
Chi Zhang https://orcid.org/0000-0003-0713-3722
Yijing Zhao https://orcid.org/0009-0004-7189-9217

References

Ali, Yasir, Md Mazharul Haque, and Zuduo Zheng. 2022. "An Extreme Value Theory Approach to Estimate Crash Risk during Mandatory Lane-Changing in a Connected Environment." *Analytic Methods in Accident Research* 33 (March): 100193. https://doi.org/10.1016/j.amar.2021.100193.

Ali, Yasir, Md. Mazharul Haque, and Zuduo Zheng. 2023. "Assessing a Connected Environment's Safety Impact During Mandatory Lane-Changing: A Block Maxima Approach." *IEEE Transactions on Intelligent Transportation Systems* 24 (6): 6639–6649. https://doi.org/10.1109/TITS.2022.3147668.

Azam, Md. Shafiul, Ashish Bhaskar, and Md. Mazharul Haque. 2022. "Driving Behaviour Modelling in the Context of Heterogeneous Traffic and Poor Lane Discipline Conditions: The State of the Art and Beyond." *Transportmetrica A: Transport Science* 18 (3): 367–434. https://doi.org/10.1080/23249935.2020.1870581.

Chen, Erdong, and Andrew P. Tarko. 2014. "Modeling Safety of Highway Work Zones with Random Parameters and Random Effects Models." *Analytic Methods in Accident Research* 1 (January): 86–95. https://doi.org/10.1016/j.amar.2013.10.003.

Cheng, Wangjun, Peng Zhang, Huibing Zhu, Xiang Shen, and Luting Ye. 2023. "Analysis of Construction Area's Impacts on Traffic Flow: A Case Study on Hangzhou Bay Bridge in China." *Physica A: Statistical Mechanics and Its Applications* 610 (January): 128393. https://doi.org/10.1016/j.physa.2022.128393.

Chowdhury, Debashish, Dietrich E. Wolf, and Michael Schreckenberg. 1997. "Particle Hopping Models for Two-Lane Traffic with Two Kinds of Vehicles: Effects of Lane-Changing Rules." *Physica A: Statistical Mechanics and Its Applications* 235 (3-4): 417–439. https://doi.org/10.1016/S0378-4371(96)00314-7.

Dehman, Amjad, and Bilal Farooq. 2023. "Capacity Characteristics of Long-Term Work Zones on Signalized Intersection Approaches." *Transportation Research Part A: Policy and Practice* 175 (September): 103791. https://doi.org/10.1016/j.tra.2023.103791.

Difei, Jing, Song Cancan, Guo Zhongyin, and Li Ran. 2021. "Influence of the Median Opening Length on Driving Behaviors in the Crossover Work Zone—A Driving Simulation Study." *Transportation Research Part F: Traffic Psychology and Behaviour* 82 (October): 333–347. https://doi.org/10.1016/j.trf.2021.09.001.

Di Pace, Roberta, Facundo Storani, Shi-Teng Zheng, Rui Jiang, and Stefano de Luca. 2024. "Calibration and Validation of a Hybrid Traffic Flow Model Based on Vehicle Trajectory Data from a Field Car-Following Experiment." *Transportmetrica B: Transport Dynamics* 12 (1): 2348592. https://doi.org/10.1080/21680566.2024.2348592.

Duan, Huiming, Xinping Xiao, Jie Long, and Yongzhi Liu. 2020a. "Tensor Alternating Least Squares Grey Model and Its Application to Short-Term Traffic Flows." *Applied Soft Computing* 89 (April): 106145. https://doi.org/10.1016/j.asoc.2020.106145.

Duan, Ke, Xuedong Yan, Xiaomeng Li, and Junyu Hang. 2023. "Improving Drivers' Merging Performance in Work Zone Using an in-Vehicle Audio Warning." *Transportation Research Part F: Traffic Psychology and Behaviour* 95 (May): 297–321. https://doi.org/10.1016/j.trf.2023.04.004.

Duan, Ke, Xuedong Yan, Xiaomeng Li, Junyu Hang, and Jingsi Yang. 2020b. "Analysis of Driver's Decision Distance and Merging Distance in Work Zone Area Based on Parametric Survival Models: With the Aid of a Driving Simulator Experiment." *Transportation Research Part F: Traffic Psychology and Behaviour* 71 (May): 31–48. https://doi.org/10.1016/j.trf.2020.03.017.

Duan, Ke, Xuedong Yan, Lu Ma, Junyu Hang, and Li. Xiaomeng. 2022. "A Multistage Analytic Model of the Longitudinal and Lateral Acceleration during Lane Changing in Work Zone Areas with the Aid of a Driving Simulator Experiment." *Transportation Letters* 14 (1): 28–38. https://doi.org/10.1080/19427867.2020.1808368.

Fei, L., H. B. Zhu, and X. L. Han. 2016. "Analysis of Traffic Congestion Induced by the Work Zone." *Physica A: Statistical Mechanics and Its Applications* 450 (May): 497–505. https://doi.org/10.1016/j.physa.2016.01.036.

Fukuda, Eriko, Jun Tanimoto, Yoshiro Iwamura, Kosuke Nakamura, and Mitsuhiro Akimoto. 2016. "Field Measurement Analysis to Validate Lane-Changing Behavior in a Cellular Automaton Model." *Physical Review E* 94 (5): 052209. https://doi.org/10.1103/PhysRevE.94.052209.

Ge, Huimin, and Yousen Yang. 2020. "Research on Calculation of Warning Zone Length of Freeway Based on Micro-Simulation Model." *IEEE Access* 8:76532–76540. https://doi.org/10.1109/ACCESS.2020.2989471.

Gu, Xin, Mohamed Abdel-Aty, Qiaojun Xiang, Qing Cai, and Jinghui Yuan. 2019. "Utilizing UAV Video Data for In-Depth Analysis of Drivers' Crash Risk at Interchange Merging Areas." *Accident Analysis & Prevention* 123 (February): 159–169. https://doi.org/10.1016/j.aap.2018.11.010.

Hang, Junyu, Xuedong Yan, Xiaomeng Li, and Ke Duan. 2022. "In-Vehicle Warnings for Work Zone and Related Rear-End Collisions: A Driving Simulator Experiment." *Accident Analysis & Prevention* 174 (September): 106768. https://doi.org/10.1016/j.aap.2022.106768.

Hou, Guangyang, and Suren Chen. 2019. "An Improved Cellular Automaton Model for Work Zone Traffic Simulation Considering Realistic Driving Behavior." *Journal of the Physical Society of Japan* 88 (8): 084001. https://doi.org/10.7566/JPSJ.88.084001.

Hou, Guangyang, and Suren Chen. 2020. "Study of Work Zone Traffic Safety under Adverse Driving Conditions with a Microscopic Traffic Simulation Approach." *Accident Analysis & Prevention* 145 (September): 105698. https://doi.org/10.1016/j.aap.2020.105698.

Huang, Lan, Zhibin Ren, and Xianghai Meng. 2024. "Changing Regularity of the Interaction Effects of Multi-Scale Factors on Drivers' Merging Behaviors in the Highway Work Zone." *Transportation Research Record: Journal of the Transportation Research Board* 2678 (8): 277–293. https://doi.org/10.1177/03611981231215334.

Huang, Zhongmin, M. N. Smirnova, Jiarui Bi, N. N. Smirnov, and Zuojin Zhu. 2023. "Analyzing Roadway Work Zone Effects on Vehicular Flow in a Freeway Ring." *International Journal of Modern Physics C* 34 (04): 2350051. https://doi.org/10.1142/S0129183123500511.

Jiang, Rui, Cheng-Jie Jin, H. M. Zhang, Yong-Xian Huang, Jun-Fang Tian, Wei Wang, Mao-Bin Hu, Hao Wang, and Bin Jia. 2017. "Experimental and Empirical Investigations of Traffic Flow Instability." *Transportation Research Procedia*, Papers Selected for the 22nd International Symposium on Transportation and Traffic Theory Chicago, Illinois, USA, 24-26 July, 2017., vol. 23 (January): 157–173. https://doi.org/10.1016/j.trpro.2017.05.010.

Knospe, Wolfgang, Ludger Santen, Andreas Schadschneider, and Michael Schreckenberg. 1999. "Disorder Effects in Cellular Automata for Two-Lane Traffic." *Physica A: Statistical Mechanics and Its Applications* 265 (3-4): 614–633. https://doi.org/10.1016/S0378-4371(98)00565-2.

Kong, Dewen, Lishan Sun, Jia Li, and Yan Xu. 2021. "Modeling Cars and Trucks in the Heterogeneous Traffic Based on Car–Truck Combination Effect Using Cellular Automata." *Physica A: Statistical Mechanics and Its Applications* 562 (January): 125329. https://doi.org/10.1016/j.physa.2020.125329.

Kummetha, Vishal C., Alexandra Kondyli, Evangelia G. Chrysikou, and Steven D. Schrock. 2020. "Safety Analysis of Work Zone Complexity with Respect to Driver Characteristics — A Simulator Study Employing Performance and Gaze Measures." *Accident Analysis & Prevention* 142 (July): 105566. https://doi.org/10.1016/j.aap.2020.105566.

Li, Shan, M. N. Smirnova, Shanjun Yang, N. N. Smirnov, and Zuojin Zhu. 2024. "Exploring the Effects of Work Zone on Vehicular Flow on Ring Freeways with a Tunnel Using a Three-Lane Continuum Model." *International Journal of Transportation Science and Technology* 14 (June): 27–41. https://doi.org/10.1016/j.ijtst.2023.03.004.

Li, Yanning, Juan C. Martínez Mori, and Daniel B. Work. 2018. "Estimating Traffic Conditions from Smart Work Zone Systems." *Journal of Intelligent Transportation Systems* 22 (6): 490–502. https://doi.org/10.1080/15472450.2018.1438274.

Liu, Jun, Qi-Lang Li, Ding-Jun Fu, and Bing-Hong Wang. 2024. "Research on a Work Zone Model with Metering Zone under Mixed Traffic Flow Environment." *International Journal of Modern Physics C* 35 (11): 2450140. https://doi.org/10.1142/S0129183124501407.

Lu, Xingyu, Li Fei, Huibing Zhu, Wangjun Cheng, and Zijie Wang. 2021. "Modeling Traffic Flow in Work Zone Sections Considering the Effect of Traffic Lights." *International Journal of Modern Physics C* 32 (09): 2150113. https://doi.org/10.1142/S0129183121501138.

Ma, Changxi, and Dong Li. 2023. "A Review of Vehicle Lane Change Research." *Physica A: Statistical Mechanics and Its Applications* 626 (September): 129060. https://doi.org/10.1016/j.physa.2023.129060.

Ma, Sen, Jiangbi Hu, and Ronghua Wang. 2023. "Impact of Transition Areas on Driving Workload and Driving Behavior in Work Zones: A Naturalistic Driving Study." *Applied Sciences* 13 (21): 11669. https://doi.org/10.3390/app132111669.

Mai, Marcus, Lei Wang, and Günther Prokop. 2019. "Advancement of the Car Following Model of Wiedemann on Lower Velocity Ranges for Urban Traffic Simulation." *Transportation Research Part F: Traffic Psychology and Behaviour*, Special TRF issue: Driving simulation, 61 (February): 30–37. https://doi.org/10.1016/j.trf.2017.08.014.

Mallikarjuna, Ch., and K. Ramachandra Rao. 2011. "Heterogeneous Traffic Flow Modelling: A Complete Methodology." *Transportmetrica* 7 (5): 321–345. https://doi.org/10.1080/18128601003706078.

Meng, Qiang, and Jinxian Weng. 2011. "An Improved Cellular Automata Model for Heterogeneous Work Zone Traffic." *Transportation Research Part C: Emerging Technologies* 19 (6): 1263–1275. https://doi.org/10.1016/j.trc.2011.02.011.

Ministry of Transport of the People's Republic of China. 2017. *JTG D20-2017: Specifications for Design of Highway Alignment*. Beijing: China Communications Press. https://xxgk.mot.gov.cn/2020/jigou/glj/202006/t20200623_3312660.html.

Morgan, J. F., A. R. Duley, and P. A. Hancock. 2010. "Driver Responses to Differing Urban Work Zone Configurations." *Accident Analysis & Prevention* 42 (3): 978–985. https://doi.org/10.1016/j.aap.2009.12.021.

Nagel, Kai, and Michael Schreckenberg. 1992. "A Cellular Automaton Model for Freeway Traffic." *Journal de Physique I* 2 (12): 2221–2229. https://doi.org/10.1051/jp1:1992277.

Oyama, Yuki, Yusuke Hara, and Takashi Akamatsu. 2022. "Markovian Traffic Equilibrium Assignment Based on Network Generalized Extreme Value Model." *Transportation Research Part B: Methodological* 155 (January): 135–159. https://doi.org/10.1016/j.trb.2021.10.013.

Raju, Narayana, Shriniwas Arkatkar, Said Easa, and Gaurang Joshi. 2022. "Customizing the Following Behavior Models to Mimic the Weak Lane Based Mixed Traffic Conditions." *Transportmetrica B: Transport Dynamics* 10 (1): 20–47. https://doi.org/10.1080/21680566.2021.1954562.

Rayaprolu, Pradeep, Sherif Ishak, Yan Qi, and Brian Wolshon. 2013. "Operational Assessment of Joint and Conventional Lane Merge Configurations for Freeway Work Zones." *Journal of Intelligent Transportation Systems* 17 (4): 255–267. https://doi.org/10.1080/15472450.2012.707052.

Schellander, Harald, Alexander Lieb, and Tobias Hell. 2019. "Error Structure of Metastatistical and Generalized Extreme Value Distributions for Modeling Extreme Rainfall in Austria." *Earth and Space Science* 6 (9): 1616–1632. https://doi.org/10.1029/2019EA000557.

Siriwardene, Sajani, Mahmud Ashraf, and Ashim Kumar Debnath. 2025. "An Observational Study of Understanding the Factors Influencing Merging Behaviour in Work Zones." *Transportation Research Part F: Traffic Psychology and Behaviour* 109 (February): 556–570. https://doi.org/10.1016/j.trf.2024.12.028.

Standardization Administration of China. 2016. *GB 1589-2016: Limits of Dimensions, Axle Load and Masses for Motor Vehicles, Trailers and Combination Vehicles*. Beijing: Standards Press of China. Available: https://openstd.samr.gov.cn/bzgk/gb/newGbInfo?hcno = 4D4FEB86F718FA6C4E2F8A0BB0EC9AC2.

Standardization Administration of China. 2017. *GB 5768.4-2017: Road traffic signs and markings — Part 4: Work zone*. Beijing: Standards Press of China. Available: https://openstd.samr.gov.cn/bzgk/gb/newGbInfo?hcno = 81495E87EE21D71FCC2759945539504F

Suh, Jonghae, and Hwasoo Yeo. 2016. "An Empirical Study on the Traffic State Evolution and Stop-and-Go Traffic Development on Freeways." *Transportmetrica A: Transport Science* 12 (1): 80–97. https://doi.org/10.1080/23249935.2015.1101508.

Toledo, Tomer, Haris N. Koutsopoulos, and Moshe E. Ben-Akiva. 2003. "Modeling Integrated Lane-Changing Behavior." *Transportation Research Record: Journal of the Transportation Research Board* 1857 (1): 30–38. https://doi.org/10.3141/1857-04.

Vieira da Rocha, Thamara, Ludovic Leclercq, Marcello Montanino, Céline Parzani, Vincenzo Punzo, Biagio Ciuffo, and Daniel Villegas. 2015. "Does Traffic-Related Calibration of Car-Following Models Provide Accurate Estimations of Vehicle Emissions?" *Transportation Research Part D: Transport and Environment* 34 (January): 267–280. https://doi.org/10.1016/j.trd.2014.11.006.

Waleczek, Helen, Justin Geistefeldt, Dijana Cindric-Middendorf, and Gerd Riegelhuth. 2016. "Traffic Flow at a Freeway Work Zone with Reversible Median Lane." *Transportation Research Procedia*, International Symposium on Enhancing Highway Performance (ISEHP), June 14-16, 2016, Berlin, vol. 15 (January): 257–266. https://doi.org/10.1016/j.trpro.2016.06.022.

Wang, Zijin, and Jaeyoung Lee. 2021. "Enhancing Construction Truck Safety at Work Zones: A Microscopic Traffic Simulation Study." *IEEE Access* 9:49750–49759. https://doi.org/10.1109/ACCESS.2021.3069275.

Weng, Jinxian, and Qiang Meng. 2015. "Incorporating work zone configuration factors into speed-flow and capacity models" *Journal of Advanced Transportation* 49 (3): 371–384. https://doi.org/10.1002/atr.1277.

Weng, Jinxian, Qiang Meng, and Tien Fang Fwa. 2014. "Vehicle Headway Distribution in Work Zones." *Transportmetrica A: Transport Science* 10 (4): 285–303. https://doi.org/10.1080/23249935.2012.762564.

Wolf, Dietrich E. 1999. "Cellular Automata for Traffic Simulations." *Physica A: Statistical Mechanics and Its Applications*, Proceedings of the 20th IUPAP International Conference on Statistical Physics, vol. 263 (1): 438–451. https://doi.org/10.1016/S0378-4371(98)00536-6.

Wu, Biao, Chunyue Zou, Yun Li, Dongnan Fan, and Shengxue Zhu. 2022b. "Impact of Road Environment on Drivers' Preference to Merging Location Selection in Freeway Work Zone Merging Areas." *Journal of Advanced Transportation* 2022 (1): 1–11. https://doi.org/10.1155/2022/2996081.

Wu, Wenjing, Yongbin Zhan, Lili Yang, Renchao Sun, and Anning Ni. 2022a. "Optimization of Lane-Changing Advisory of Connected and Autonomous Vehicles at a Multi-Lane Work Zone." *International Journal of Modern Physics C* 33 (02): 2250020. https://doi.org/10.1142/S0129183122500206.

Yamauchi, Atsuo, Jun Tanimoto, Aya Hagishima, and Hiroki Sagara. 2009. "Dilemma Game Structure Observed in Traffic Flow at a 2-to-1 Lane Junction." *Physical Review E* 79 (3): 036104. https://doi.org/10.1103/PhysRevE.79.036104.

Yang, Da, Xiaoxia Zhou, Gang Su, and Sijing Liu. 2019. "Model and Simulation of the Heterogeneous Traffic Flow of the Urban Signalized Intersection With an Island Work Zone." *IEEE Transactions on Intelligent Transportation Systems* 20 (5): 1719–1727. https://doi.org/10.1109/TITS.2018.2834910.

Yeom, Chunho, William Rasdorf, Nagui Rouphail, and Bastian Schroeder. 2018. "Simulation of Work Zones with Lane Closures in Proximity of Freeway Interchanges." *IEEE Intelligent Transportation Systems Magazine* 10 (3): 184–195. https://doi.org/10.1109/MITS.2018.2842027.

Zhang, Chi, Bo Wang, Shaoxiang Yang, Min Zhang, Quanli Gong, and Hong Zhang. 2020. "The Driving Risk Analysis and Evaluation in Rightward Zone of Expressway Reconstruction and Extension Engineering." *Journal of Advanced Transportation* 2020 (1): 1–13. https://doi.org/10.1155/2020/8943463.

Zhang, Jian, Xiling Li, Rui Wang, Xiaosi Sun, and Xiaochao Cui. 2012. "Traffic Bottleneck Characteristics Caused by the Reduction of Lanes in an Optimal Velocity Model." *Physica A: Statistical Mechanics and Its Applications* 391 (7): 2381–2389. https://doi.org/10.1016/j.physa.2011.11.045.

Zhang, Yifan, Qian Xu, Jianping Wang, Kui Wu, Zuduo Zheng, and Kejie Lu. 2023ba. "A Learning-Based Discretionary Lane-Change Decision-Making Model With Driving Style Awareness." *IEEE Transactions on Intelligent Transportation Systems* 24 (1): 68–78. https://doi.org/10.1109/TITS.2022.3217673.

Zhang, Yue, Yajie Zou, Yangyang Wang, Lingtao Wu, and Wanbing Han. 2023bb. "Understanding the Merging Behavior Patterns and Evolutionary Mechanism at Freeway On-Ramps." *Journal of Intelligent Transportation Systems* 27 (5): 573–586. https://doi.org/10.1080/15472450.2022.2069501.

Zhang, Zhuoran, Burcu Akinci, and Sean Qian. 2023aa. "How Effective Is Reducing Traffic Speed for Safer Work Zones? Methodology and a Case Study in Pennsylvania." *Accident Analysis & Prevention* 183 (April): 106966. https://doi.org/10.1016/j.aap.2023.106966.

Zheng, Lai, and Tarek Sayed. 2019. "From Univariate to Bivariate Extreme Value Models: Approaches to Integrate Traffic Conflict Indicators for Crash Estimation." *Transportation Research Part C: Emerging Technologies* 103 (June): 211–225. https://doi.org/10.1016/j.trc.2019.04.015.

Zheng, Shi-Teng, Rui Jiang, Bin Jia, Junfang Tian, Marouane Bouadi, Michail A. Makridis, and Anastasios Kouvelas. 2023a. "A Parsimonious Enhanced Newell's Model for Accurate Reproduction of Driver and Traffic Dynamics." *Transportation Research Part C: Emerging Technologies* 154 (September): 104276. https://doi.org/10.1016/j.trc.2023.104276.

Zheng, Shi-Teng, Michail A. Makridis, Anastasios Kouvelas, Rui Jiang, and Bin Jia. 2023b. "A Multi-Objective Calibration Framework for Capturing the Behavioral Patterns of Autonomously-Driven Vehicles." *Transportation Research Part C: Emerging Technologies* 152 (July): 104151. https://doi.org/10.1016/j.trc.2023.104151.

Zheng, Zuduo. 2014. "Recent Developments and Research Needs in Modeling Lane Changing." *Transportation Research Part B: Methodological* 60 (February): 16–32. https://doi.org/10.1016/j.trb.2013.11.009.

Zhu, H. B., N. X. Zhang, and W. J. Wu. 2015. "A Modified Two-Lane Traffic Model Considering Drivers' Personality." *Physica A: Statistical Mechanics and Its Applications* 428 (June): 359–367. https://doi.org/10.1016/j.physa.2015.02.016.

Zhu, Wenxing, Lei Jia, and Liang Zhao. 2010. "Modeling and Simulation of Traffic Flow in Work Zone on Highway." 2010 *8th World Congress on Intelligent Control and Automation*, July 2010, 471–476. https://doi.org/10.1109/WCICA.2010.5553793.. 471 476 >

Appendix

Table A1. Statistics of DMLC position probability distribution function parameter estimation.

Case	DMLC position probability distribution	Transition area length(m)	Mean(m)	Variance	Parameter estimation			Log-Likelihood value	AIC	BIC
					μ (SD)	σ (SD)	k (SD)			
A	EV	190.31	156.5	1812.7	217.140(7.4403)	104.978(4.9982)	/	1383.43	2770.86	2770.86
	GEV		164.5	7414.5	122.964(6.7441)	87.949(4.9134)	-0.118(0.0575)	1348.6	2703.20	2703.20
B	EV		178.8	20394.7	243.027(7.8846)	111.349(5.4207)	/	1400.06	2804.12	2812.52
	GEV		185.4	11829.4	142.888(7.8647)	103.016(5.7222)	-0.195(0.0570)	1374.59	2755.18	2761.58
C	EV		218.6	16638.2	276.686(7.1189)	100.572(4.8701)	/	1376.91	2757.82	2766.09
	GEV		225.3	9955.5	188.547(7.2568)	98.000(5.1120)	-0.248(0.0458)	1355.34	2716.68	2722.95
D	EV	82.53	112.6	10447.0	158.561(9.6137)	79.693(6.3521)	/	456.773	917.55	925.83
	GEV		121.4	6755.2	87.2732(6.0970)	46.283(4.8709)	0.187(0.1084)	430.809	867.62	873.90
E	EV		109.3	13217.8	160.992(10.811)	89.641(6.9467)	/	464.858	933.72	941.78
	GEV		119.5	6701.8	81.855(6.9089)	53.630(5.2814)	0.113(0.0944)	439.07	884.14	890.21
F	EV		111.3	15914.8	168.093(10.869)	98.362(6.9976)	/	562.826	1129.65	1137.94
G	EV	164.72	141.6	10581.8	187.911(11.614)	80.206(7.8660)	/	317.522	639.04	647.54
	GEV		147.7	5743.6	113.745(9.2732)	59.976(6.7747)	-0.012(0.1115)	306.309	618.62	625.11
H	EV		152.8	13651.5	205.418(13.196)	91.100(9.0615)	/	324.705	653.41	662.36
	GEV		159.8	8482.8	117.392(9.5210)	61.621(7.2529)	0.101(0.1135)	311.223	628.45	635.39
I	EV	172.62	175.8	20109.1	237.655(12.086)	110.566(7.8909)	/	586.838	1177.68	1186.61
	GEV		185.2	9295.6	141.640(8.4641)	74.131(6.0947)	0.011(0.0714)	559.85	1125.70	1132.63
J	EV		179.5	22757.8	247.354(12.850)	117.623(8.6219)	/	594.263	1192.53	1201.31
	GEV		190.1	13241.7	137.134(8.9671)	76.404(6.8536)	0.105(0.0887)	568.076	1142.15	1148.94
K	EV		164.1	16504.0	221.888(10.842)	100.166(6.9603)	/	588.517	1181.03	1190.00
	GEV		175.4	7221.9	136.353(6.3569)	56.988(4.7343)	0.100(0.0656)	551.224	1108.45	1115.41
L	EV	225	224.1	3737.2	271.637(4.0454)	47.665(3.1363)	/	837.163	1678.33	1683.25
	GEV		242.7	4190.2	232.809(6.0404)	70.348(5.0277)	-0.679(0.0478)	832.009	1670.02	1672.94